# EVALUATING CHANNEL MIGRATION OF THE LOWER GUADALUPE RIVER: SEGUIN, TX TO THE SAN ANTONIO RIVER CONFLUENCE

A Thesis

by

TAYLOR ROWLEY

Submitted to the Office of Graduate and Professional Studies of
Texas A&M University
in partial fulfillment of the requirements for the degree of

MASTER OF SCIENCE

| | |
|---|---|
| Chair of Committee, | John R. Giardino |
| Committee Members, | Peter S. K. Knappett |
| | John D. Vitek |
| Head of Department, | Ronald Kaiser |

December 2016

Major Subject: Water Management and Hydrological Science

# ABSTRACT

On Earth, rivers are found meandering across the landscape. To accommodate dynamic flow regimes and sediment loads, rivers are in constant adjustment within the channel and adjacent valley. Extreme floods as well as base flows alter the course of the river at different rates. Geomorphic characteristics control the extent of adjustment of a river over time. Numerous geomorphic and watershed characteristic variables influence the course of the river at different spatial and temporal scales. Each river is unique, and each reach of river is different from another, thus, the mechanisms driving, and the rates of changing the course of one river reach may not be the same for another.

This study addresses the change and driving mechanisms on a 380 km reach of the Guadalupe River, from Seguin, TX to the confluence with the San Antonio River. The following questions are addressed: (1) at what rate does channel migration occur along the lower Guadalupe River, and (2) what are the driving mechanisms controlling channel migration? To determine the answers, a Geographic Information System (GIS) analysis was performed using data from 1960 to 2014. An analysis of the 380 km reach was performed as well as a sub-reach analysis of seven reaches.

Statistical analysis was performed for the entire reach and the sub-reaches and shows that the channel is relatively stable. For the 380 km reach, lateral rates of migration range from 0.11 to 1.65 m/yr with a mean of 0.36 m/yr. To understand the drivers of lateral migration, sub-reach analysis concluded that presence of vegetation and high silt-clay soil composition relate to lower rates of migration.

Each zone varied significantly from one another. The highest and lowest average rates of migration occur in adjacent zones, the Upper and Middle Deltas (UD, MD) and the Belmont Fault zone (BFZ) and Upper Coastal Plain (UCP). Several dams outside of and within the study reach influence the BFZ and UCP, whereas an active zone of subsidence in this area contribute to migration in the UD and MD.

# ACKNOWLEDGEMENTS

This thesis is the result of a push from my former undergraduate advisor for planting the seed that I was more than capable of completing a Master's degree. I am appreciative of all of the people I have met and experiences I have had to bring me to this point.

I am indebted to my committee chair and advisor Dr. Giardino, for taking a chance on me not once, but twice. The opportunities he continually provides have gotten me where I am today. I appreciate his influence on me as an academic and his way of passively pushing me forward, for without him, I would be lost. I would also like to thank my committee member Dr. Knappett for providing guidance along this journey as well as letting me join your group as a part time member. I thank you for always letting me lend a hand on your projects and field excursions of all varieties. I thank Dr. Vitek for serving as a voice of reason and for understanding the greatness that is Oklahoma.

I want to also thank my colleagues at the Oklahoma Water Resources Board for unknowingly guiding me down this path. Specifically, Monty Porter, who shared a love for data, and Jason Murphy for infinite support and encouragement.

Thank you to the Water Program, Department of Geology and Geophysics, Texas A&M University, and the Texas Water Development Board for helping to fund me through my program.

I thank friends and colleagues for providing sanity through this experience, and finally I give thanks to an extremely supportive family for providing unconditional love, support, and patience.

# CONTRIBUTORS AND FUNDING SOURCES

## Contributors

This work was supervised by a thesis committee consisting of Dr. Rick Giardino, my advisor, and Dr. Peter Knappett the Department of Water Management and Hydrological Sciences and Dr. John Vitek of the Department of Geology and Geophysics.

## Funding Sources

Graduate study was supported by a grant from the Texas Water Development Board and the Department of Water Management and Hydrological Sciences at Texas A&M University.

TABLE OF CONTENTS

Page

LIST OF FIGURES

Page

LIST OF TABLES

Page

# 1. INTRODUCTION

## *1.1 Context*

River meanders are the manifestation of events resulting in instability, which occur along the river-channel boundary. Instability in alluvial streams is the result of two driving aspects of the velocity of water and sediment transport. If both of these are sufficiently robust, sediment transport along the bottom of the channel will swing from the center of the river to one side or the other of the river channel, producing a helical flow pattern.

A helical flow pattern increases the deposition along the one side of the channel where water velocities are decreased, whereas faster flows erode the opposite bank. Additionally, the water is deflected through the expanding bend toward the opposite bank of the channel further downstream and triggers the growth of a new bend. Through this meander process, sediment-flow instability is sufficiently strong to form alternate bars in the relatively straight channel. Bank erosion occurs on alternate sides of the channel, which is encouraged by sediment deposits forming bars opposite bank erosion. The result of this alternating pattern of bank erosion and bar deposition is the creation of a meandering river pattern.

One must understand that for a meandering channel to develop, the banks of the stream must be sufficiently cohesive to facilitate maintenance of a reasonably uniform width as the channel is deformed into a series of bends and reaches. Bank materials consisting of fine silts and clays as well as the root systems of plants provide the

necessary cohesion. If the cohesion is insufficient, however, channel instability can initiate bifurcation of the river into two or into multiple channels.

A river will react to channel instability to achieve a state of dynamic equilibrium where sediment load is balanced with discharge and stream gradient inducing minimal erosion and deposition (Bridge, 2009; Church, 2010). Dynamic equilibrium is a balance within the entire river system. A river is dynamically stable once in dynamic equilibrium because it has the ability to react to a range of disturbances through self-repair mechanisms (Langbein and Leopold, 1964; Knighton, 2014; WADOE, 2016).

Dynamic equilibrium is a fundamental geomorphic concept. River managers, engineers, and geomorphologists base much of their management of rivers on the concept. Although generally accepted in geomorphology, the concept of dynamic equilibrium has been questioned and critiqued for decades (Ahnert, 1994; Bracken and Wainwright, 2006; Lewin, 2016). Phillips (2007) has provided examples of several Texas Coastal Plain rivers that do not follow the concept. Phillips, unfortunately, does not include information on the Guadalupe River, so the equilibrium status of the river is unknown. We assume that the lower Guadalupe River does follow the equilibrium concept because of the shape of the longitudinal channel profile. Phillips (2007) questions the equilibrium of rivers that have a convex profile, but the reach of the lower Guadalupe tends toward linear.

Concave and convex longitudinal profiles are a result of erosion and deposition throughout the channel as the river flows downstream. Sediment exchange is fundamental to river dynamics, however, the amount of exchange of sediment as well as

the length of time has important implications for the dynamics of a river (TIFP, 2010). Discharge directly affects sediment load and this is often regulated through human intervention (Phillips, 2012). To regulate discharge, structures such as dams or point-source dischargers must comply with flow regulations and limitations to minimize disturbance up and downstream. Regulatory programs have been created to establish the ideal rate of discharge to promote ecological health of a river while maintaining beneficial uses for various stakeholders.

The purpose of this present study is to determine and explain meander migration as a response to geomorphic parameters that occur along the length of the lower Guadalupe River so that river managers and stakeholders can understand the dynamic controls of the river. Documenting evidence of river stability will compliment prior work (Holley, 1992; Perkin and Bonner, 2011; Phillips, 2007; 2011; 2012; Phillips and Slattery, 2007), and also provide the scientific basis for instream-flow recommendations for this segment of river. Figure 1 presents the Guadalupe River Basin and study area.

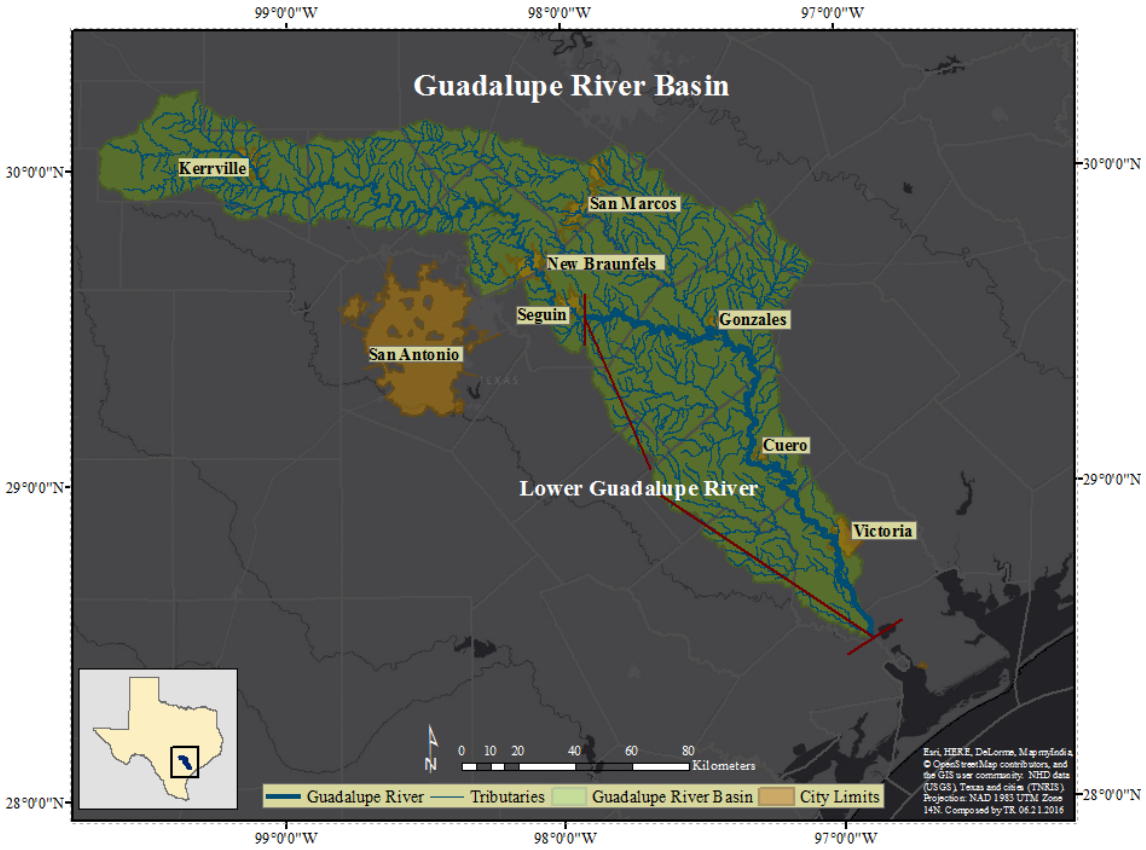


**Figure 1. Guadalupe River Basin with the lower Guadalupe River study area highlighted.**

*1.2 Objectives*

The purpose of this thesis is to present an analysis on historic channel migration of the lower Guadalupe River. To accomplish this, two objectives were determined:

1.) Calculate rates of meander migration along selected reaches of the Guadalupe River.

2.) Determine the driving mechanisms controlling channel migration.

*1.3 Significance*

This research has two contributions. First, the research provides a scientific explanation of cause and rate of meander migration on the lower Guadalupe River, which will contribute to the body of knowledge on meander migration. Second, the scientific explanation of meander migration can be used by the various stakeholders on the management of the river. This study will provide an overview of the entire lower Guadalupe River and its stability. Selected reaches will be analyzed to gain a perspective at multiple spatial and temporal scales. As a result, the river will be understood as a system rather than an individual element at one point in time.

# 2. BACKGROUND

## *2.1 River Development and Scale*

River development is dependent on autochthonous and allocthonous controls that influence what authors Leopold and Wolman (1957) note about river channel morphology; rivers are straight, meandering, or braided. Rivers migrate across an alluvial floodplain as sediment is eroded from one location and deposited in another. Rivers migrate laterally and vertically. The morphology of a river is primarily dependent on channel slope and discharge relationships. Because other factors play a role in influencing the morphology of a river, numerous classification schemes have been created to explain the additional controls that are operational across multiple scales.

Whereas numerous approaches have been created, I highlight six different approaches only. Schumm (1963) relates river adjustment to sediment load and transport mechanisms, as well as to the local geology, rather than specific channel hydraulics. Frissell et al. (1986) view the river in the context of the whole watershed by using a hierarchical framework and systems' approach. Montgomery and Buffington (1997), on the other hand, classify a river in terms of changes in morphology at the reach scale. They identify changes in riparian vegetation and hillslope process to determine best-fit reaches. Brierly and Fryirs (2000; 2013) take a completely different view by using a bottom-up approach to identify present landforms. They first assess the morphodynamics of the landforms and then interpret the evolution of the river and its catchment, which are the result from these dynamics. Lastly, Gurnell (2014) uses the presence of instream

and riparian vegetation to understand stability, whereas Wohl (2013) uses woody debris to explain controls of geomorphic change.

The six examples explain controls and different ways of understanding geomorphic change; each at different spatial scales. Definition of geomorphic change is dependent on the scale of the questions being asked. As Tobler (1970, 236) said, "Everything is related to everything else, but near things are more related than distant things." The analysis of a river is dependent on scale; hence, the reason why so many classification schemes have been created. A scientist must determine a best approach to use to answer the question being asked.

*2.2 Weather and Climate*

Once a best approach to classify the geomorphology of a river is determined, other factors influencing the evolution of a river must be considered. Climate and weather have a direct impact on the flow regime of a river. Precipitation can lead to runoff, resulting in an increase of discharge to a river. An increase in discharge, increases the stream power, which is the capacity for flowing water to perform geomorphic changes through sediment transport (Phillips and Slattery, 2007; Bizzi and Lerner, 2015). Stream power can be expressed as:

$$\boldsymbol{\Omega = \gamma Q_{\mu} S} \qquad \text{Eq. (1)}$$

where $\Omega$ is stream power, $\gamma$ is the specific weight of water (9810 $N/m^3$), $Q_\mu$ is the mean daily peak flow, and S is slope. Increased stream power is a result of higher discharge; thus, an increase in geomorphic work is expected.

Baker (1977) provides an example of this phenomenon on the upper Guadalupe River. The author states that a threshold must be exceeded by an applied stress for geomorphic work to occur. When stream power increases, thresholds for sediment transport are exceeded. The higher the threshold, the higher the stream power needs to be. Baker observes the result of exceeding a threshold after a flood in 1972 near New Braunfels, TX. He cited as evidence of the flood, large boulders transported downstream, limestone joints plucked from the channel bed, erosion of cut banks, and large scour holes. Figure 2 shows the middle Guadalupe River Basin, including the New Braunfels area.

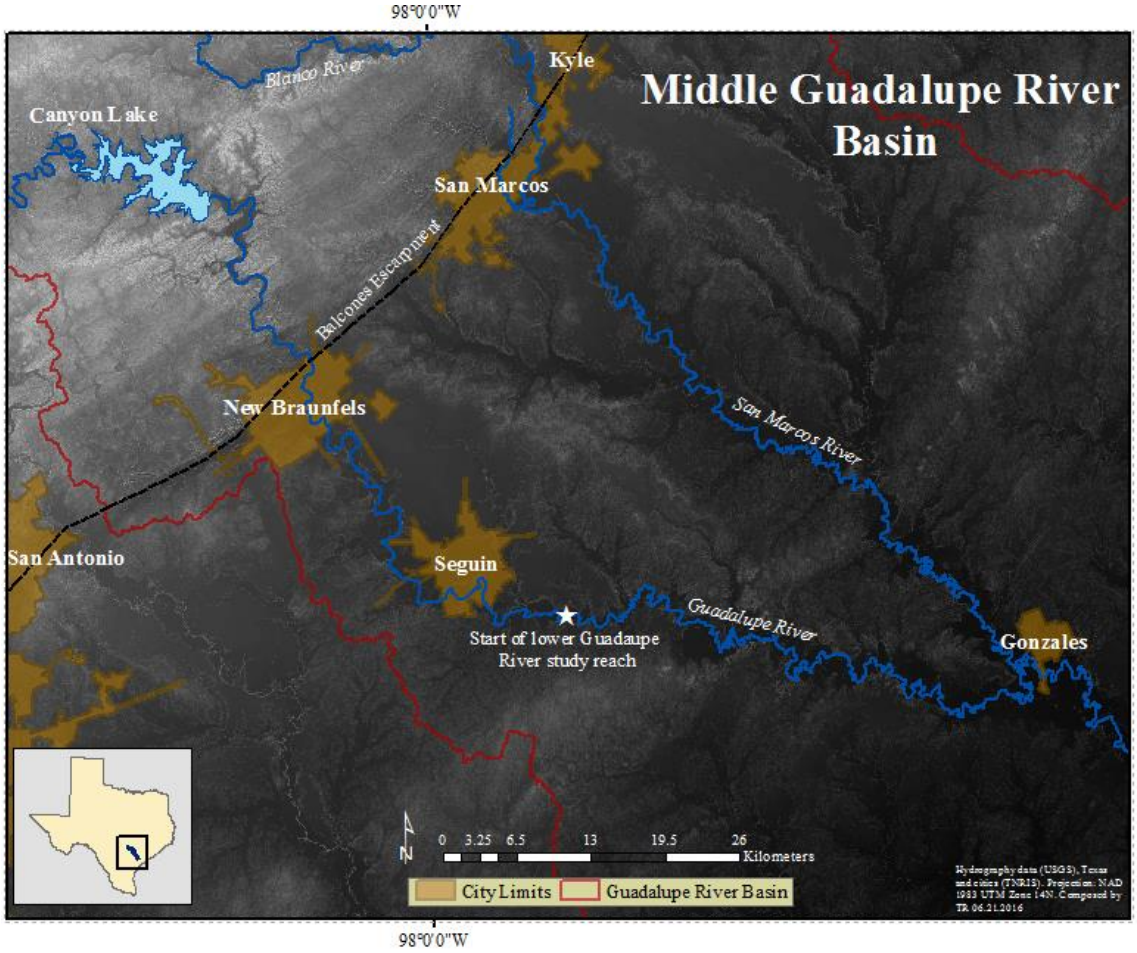


**Figure 2. Middle Guadalupe River Basin including Canyon Lake, the Balcones Escarpment and major tributaries to the Lower Guadalupe River.**

Large floods have shaped the upper portion of the river through the Edwards Plateau and the Balcones Escarpment. Limestone and lack of vegetation in this physiographic region, along with the local climatic influences allow for extreme rates of runoff that increase stream power which entrain sediments and help carve the channel of the upper Guadalupe River.

Weather in the region are the result of an abrupt topography change that creates an orographic effect ideal for rapid convective thunderstorm development and torrential rains (Dorroh, 1946). Baker (1975) also notes that storms with a tropical origin can have severe impact if the front reaches the orographic barrier of the escarpment. Longer duration rains persist and create floods resembling the September 1921 storm in which 970 mm of rain fell in 24 hours; one of the greatest magnitude storms in the contiguous U.S. (Baker, 1975). More recently, the region has experienced severe flash flooding, setting record stage heights and discharge volumes in May and October 2015.

The May and October 2015 storms directly affected the upper Guadalupe River, but the effects were dampened as a result of water retention in Canyon Lake. The lower section of the river was indirectly affected downstream of the confluence of the San Marcos River near Gonzales, TX. The San Marcos River was affected by the same storm, however, no major dams for flood control exist on the river, only low head dams for flow regulation at lower discharges. Lack of flood control structures enhance the propagation of flood waves to directly affect the Guadalupe River below the confluence. As flood waves propagate downstream, increasing discharge has the potential to reshape the channel of the lower Guadalupe River.

### *2.3 Dams*

Flood waves also propagate downstream as a result of water storage and hydropower generation at Canyon Lake dam. Dams regulate flows downstream, especially those used for hydropower. Daily releases made to meet energy needs result

in hydropeaking in the hydrograph. These resulting pulses induce irregular flow regimes that raise low flows, and dampen flood peaks (Magilligan and Nislow, 2005; Graf, 2006).

Wolman and Miller (1960) explain that landscapes are modified by frequent moderate flows rather than rare catastrophic floods. The authors observed this in the wet and humid climate of the east coast. Although they did not consider dams to be the cause of a moderate flow regime, their description that this type of flow regime dominates geomorphic changes applies in this regulated reach of the Guadalupe River.

### *2.4 Geomorphic and Watershed Characteristics*

Flow regime, among numerous other factors, control channel changes in the lower Guadalupe River. A Texas Water Development Board study conducted by Phillips (2011) looked at geomorphic boundaries and transition zones linked to specific geomorphic controls of the entire length of the Guadalupe River. The author outlined seven controls including slope, sinuosity, geology, valley confinement, valley width, floodplain-river connectivity, and flow regime. Each control has its own set of boundary points along the stretch of the river delineated by GIS analysis of DEMs (Digital Elevation Model) and aerial imagery. Visual indicators such as dams, recent avulsions, and oxbow density aided boundary determinations.

The use of geomorphic boundary zones to assess channel migration and mechanisms of change was chosen as a result of improving on previous studies. A similar study, examining rates of migration on the lower Brazos River in Texas, was

conducted by Lee and Giardino (2011). The study used counties as boundaries for reach delineation. Counties are not typically determined by Earth surface properties, thus, boundaries that account for these properties should be used. Another study performed on the Brazos River by Gillespie and Giardino (1997) used tributary confluences to determine reach boundaries. Richard et al. (2005) also used channel characteristics including confluences, degree of meandering or braiding, presence and manmade controls, and channel confinement to denote reach boundaries for their study of lateral migration downstream of Cochiti Dam, NM.

### *2.5 Channel Pattern and Geometry*

The previous studies used geomorphic-related reach boundaries as well as watershed and channel planform variables to analyze lateral rates of migration. Gillespie and Giardino (1997) and Richards (2005) used variables including radius of curvature, arc length, channel width, amplitude, and sinuosity as indicators of lateral migration. These indicators are analyzed in association with variables including discharge, stream power, sample median grain sizes, and vegetation to identify driving mechanisms of change. Other studies point to a more specific driver of channel change. For example, Nicoll and Hicken (2010) focused on valley confinement as the specific driver of lateral migration in several Canadian Prairie rivers, and Konsoer et al. (2016) used riparian vegetation and bank material heterogeneity as the driving mechanisms for movement of meander bends.

Channel geometry and pattern are variables known to affect and influence lateral movement of meander bends. Channel patterns vary across and within river systems as the channel approaches dynamic equilibrium. As a river adjusts to a specific base level, channel patterns change (Schumm et al., 2002 , Cyr and Granger, 2008 ). Channel pattern can be used as a measurement to understand the stability of the river. Sinuosity, or the ratio between channel and valley length, is one characteristic commonly used. Schumm (1963) relates sinuosity to river patterns, and he classified these into five categories: straight (1-1.3), transitional (1.3-1.7), regular (1.7-1.8), irregular (1.8-2.3), and torturous (>2.3).

Channel geometries also vary. The quantification of various geometries can serve as additional indicators of the stability of the river. In a meandering system, distinct relationships are present between channel planform characteristics including width, wavelength, and radius of curvature of meanders (Leopold, 1994). The wavelength between two meanders averages eleven times the average width of the channel, and the radius of curvature is generally one fifth of the wavelength.

### 2.5.1 Radius of Curvature

Radius of curvature is an important parameter when analyzing lateral migration; 9the result of shear stress acting on the outside bank of a meander bend. Figure 3 provides a diagram of the mechanics of lateral migration in a meander bend.

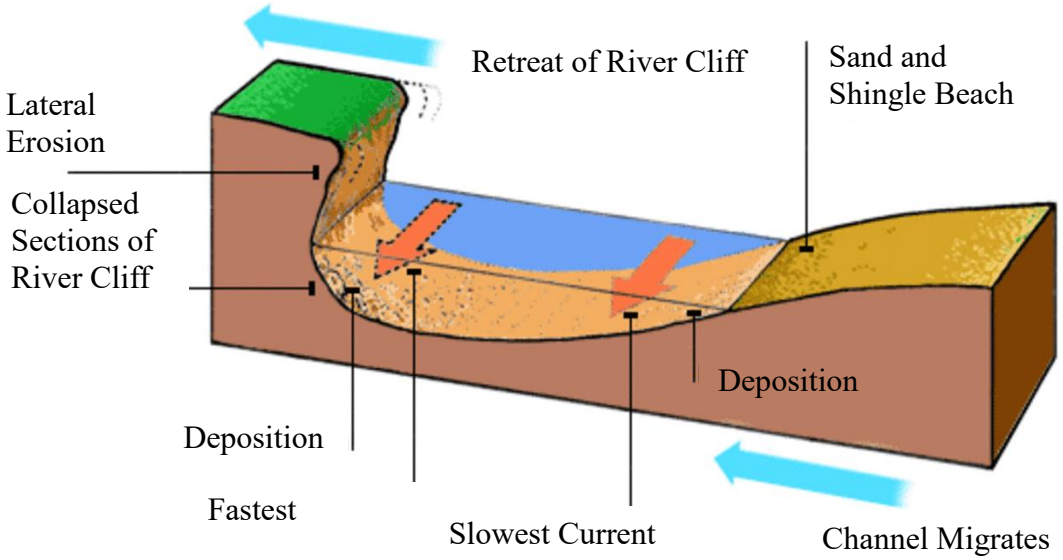


**Figure 3. Cross-section of the process of lateral migration in a meander bend (Modified from www.bbc.co.uk/bitesize/higher/geography/physical/hydrosphere/revision/3/).**

During high discharges, meander bends migrate laterally as the bend is eroded by increased shear stresses that destabilize the bank (Briaud, 2001; Darby et al. 2002, Wallick et al., 2006). Shear stress is controlled by flow velocities in the channel as well as the channel geometry and bank material. Leopold and Wolman (1957) suggest that radius of curvature, or tightness of a bend, relates to lateral migration. To scale the radius to channel size, a ratio of radius and average channel width is often used.

The tightness of the bend relates to the resistance of the outside bank to erosion. Bagnold (1960) suggests that resistance is lowest at a ratio of ~2. When values are less than two, the flow loses force and does not directly impact the outside bend. At values

greater than two, the bend is less “tight” and results in a higher resistance on the outside bend. Figure 4 displays the difference in channel pattern for a variety of ratio values.

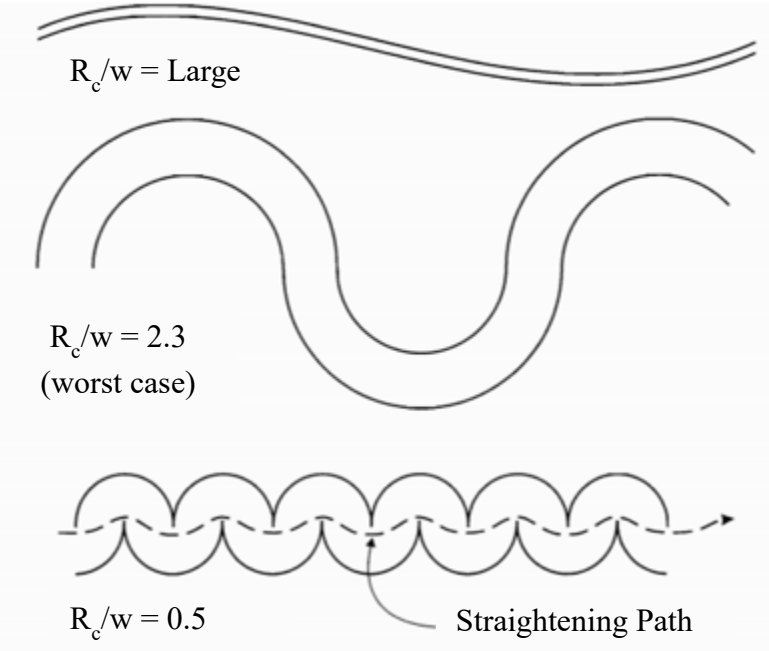


**Figure 4. Rivers with various radii of curvature and their shape where $R_c$ = radius of curvature and w = channel width (Modified from Briaud et al., 2001.).**

Nanson and Hickin (1983; 1984; 1986) test Bagnold’s theory in a field setting on several rivers of the Canadian Prairie in British Columbia. They compare rates of lateral migration to values of the ratio of radius of curvature and channel width. They find a strong relationship exists between the highest rates of lateral migration in the dataset and ratio values between two and three. Values less than two and greater than three relate to lower rates of migration, therefore, the authors determine the ratio of radius of curvature

and channel width to be used as an indicator of meander stability. Unfortunately, the rivers of the Canadian Prairie are not applicable to the rivers in Texas. To determine if Texas rivers also follow the same trends as the rivers of the Canadian Prairie, my study attempted to understand if the ratio holds true for rivers of Texas.

# 3. STUDY AREA

## *3.1 Watershed Characteristics and Geomorphology*

The headwaters of the Guadalupe River are located in near Kerrville in Kerr County, Texas where the river forms from groundwater springs and flows east on the Edwards Plateau before dropping through the Balcones Escarpment and turning southeast, where it flows toward the San Marcos River confluence near Gonzales, TX. Here it flows south for 280 km through the Gulf Coastal Prairie before draining into Guadalupe Bay in the Gulf of Mexico. The Guadalupe River drainage area is ~15,418 $km^2$ and has a river length of ~ 658 km (TSHA, 2010). This study will evaluate a ~380 km section from the USGS gauge at US HWY 1117 in Seguin, TX to the confluence of the San Antonio River, 11 km before the Gulf of Mexico. Refer to Figure 1 for a map of the Guadalupe River Basin.

Previous work conducted by Phillips (2011) designated geomorphic boundary thresholds along the Guadalupe River. From the thresholds, geomorphic zones were delineated. Seven zones are found within the lower Guadalupe River study area. Figure 5 shows the seven delineated geomorphic zones, Table 1 includes the zones and the associated coordinates, and Table 2 provides characteristics of each zone.

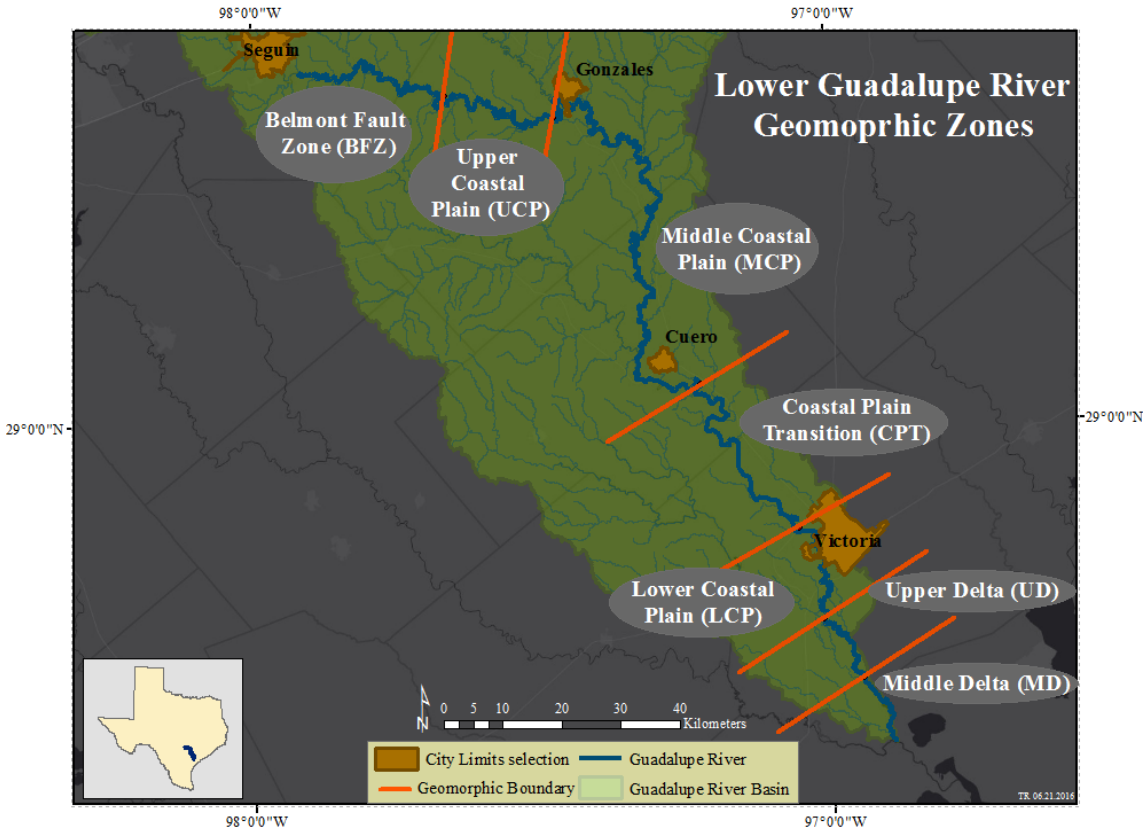


**Figure 5. Map including study reach and associated study sub-reaches by geomorphic zone.**

**Table 1. Geomorphic zones and associated geographic coordinates using the geographic coordinate system North American Datum 1983.**

| Geomorphic Zone | Distance from Gulf (km) | Reach Distance (km) | Latitude | Longitude |
|---|---|---|---|---|
| **Belmont Fault Zone** | 376 | 79 | 29.503 | -97.663 |
| **Upper Coastal Plain** | 327 | 35 | 29.469 | -97.472 |
| **Middle Coastal Plain** | 287 | 40 | 29.058 | -97.222 |
| **Coastal Plain Transition** | 130 | 157 | 28.836 | -97.054 |
| **Lower Coastal Plain** | 78 | 52 | 28.698 | -97.013 |
| **Upper Delta** | 40 | 38 | 28.608 | -96.946 |
| **Middle Delta** | 11 | 29 | 28.506 | -96.84 |

**Table 2. Characteristics of geomorphic zones adapted from Phillips (2011).**

| Geomorphic Zone | Slope | Sinuosity | Valley Width (km) | Valley Confinement | CFC | Geology |
|---|---|---|---|---|---|---|
| **Belmont Fault Zone** | $6.5 \times 10^{-4}$ | 3.07 | 1.4-2.1 | Partially Confined | Moderate | Eocene; Carrizo Sand and Recklaw |
| **Upper Coastal Plain** | $6.1 \times 10^{-4}$ | 2.38 | 0.9-3.5 | Partially Confined | Moderate | Eocene; Carrizo Sand |
| **Middle Coastal Plain** | $2.7 \times 10^{-4}$ | 2.87 | 0.8-7.1 | Partially Confined | Moderate | Eocene |
| **Coastal Plain Transition** | $3.7 \times 10^{-4}$ | 1.73 | 1-2.8 | Partially Confined | High | Miocene, Pliocene |
| **Lower Coastal Plain** | $3.3 \times 10^{-4}$ | 2.49 | 4.5-5.5 | Unconfined | High | Qt Lissie and Beamont |
| **Upper Delta** | $5.9 \times 10^{-5}$ | 2.13 | 5.0-6.0 | Unconfined | Very High | Holocene Delta, Qt Beaumont |
| **Middle Delta** | $1.9 \times 10^{-4}$ | 1.39 | 6.0-7.0 | Unconfined | Very High | Holocene Delta, Qt Beaumont |

Lateral rates of migration were assessed for the entire reach as well as in each sub-reach. A description of each zone, upstream to downstream, is provided below; adapted from Phillips (2011).

### 3.1.1 Zone 1 – Belmont Fault Zone (BFZ)

The reach starts at the FM 1117 bridge, east of Seguin, TX, and extends 55 km to the top of zone 2. This zone has tortuous meanders and straight segments, often parallel with mapped faults near Belmont. Geologic changes constrain the river in this reach. The valley widens where the Carrizo Sand Formation outcrops, whereas the more

resistant Recklaw formation confines the lower valley. Regular dam releases from Canyon Lake dominate the flow through this reach. Figure 6 shows the Belmont Fault Zone sub-reach.

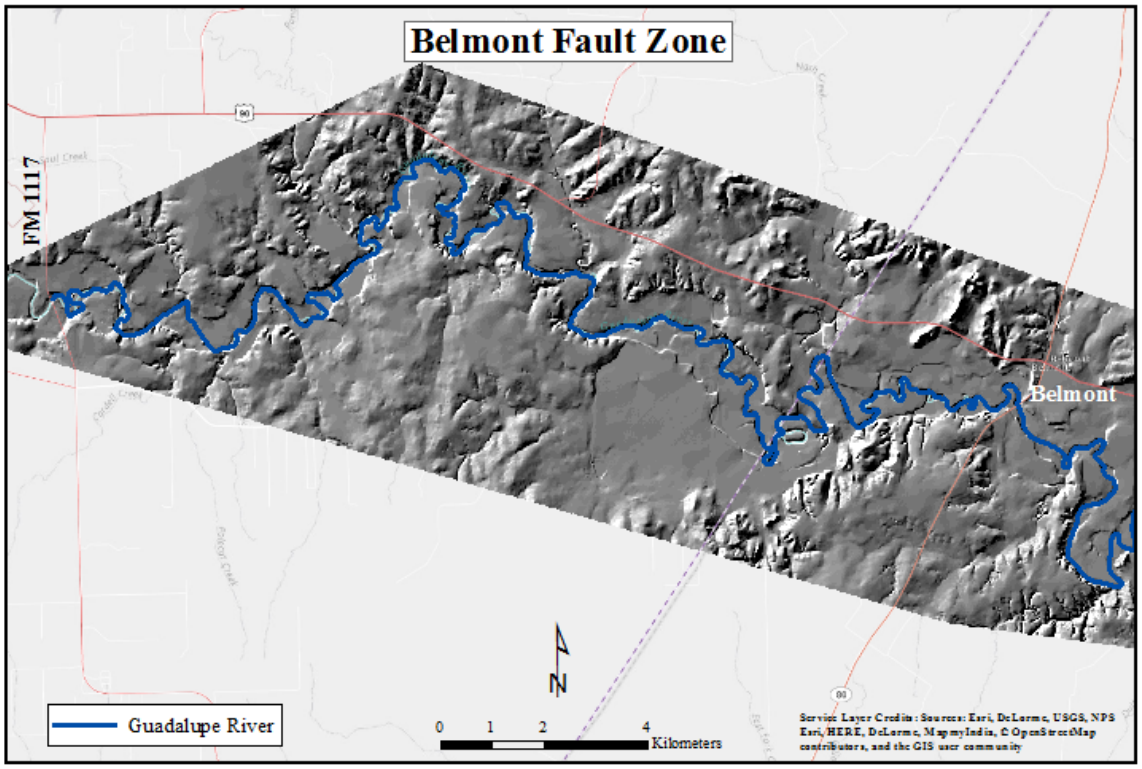


**Figure 6. Map of the Belmont Fault Zone geomorphic zone and sub-reach.**

### 3.1.2 Zone 2 – Upper Coastal Plain (UCP)

The upper coastal plain starts near Belmont, TX and extends 44 km to the San Marcos River confluence. The reach has the highest sinuosity and slope of all zones within the study reach. The valley is partially confined and less variable than in zone 1.

Zone 2 has several small hydroelectric dams that control flow, but is highly influenced by Canyon Lake reservoir as well as the Comal and San Marcos Rivers. The reach includes two reservoirs, Lake Gonzales and Wood Lake. Figure 7 provides a map of the zone.

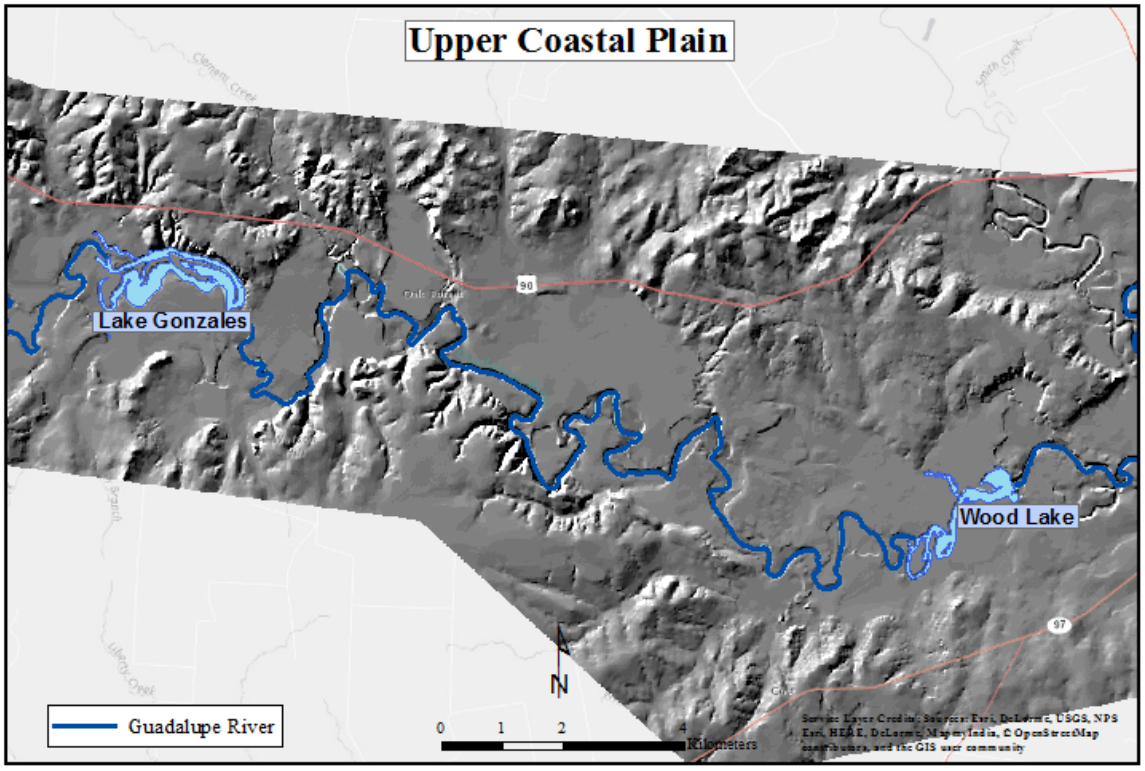


**Figure 7. Map of the Upper Coastal Plain geomorphic zone and sub-reach.**

### 3.1.3 Zone 3 – Middle Coastal Plain (MCP)

Zone 3 is the longest reach flowing 147 km from the confluence with the San Marcos River to just downstream of Cuero, TX. The reach is partially confined with variable valley widths. Sinuosity is lower than the surrounding up and downstream reaches. Again, the Carrizo Sand Formation dominates the wider valley sections, whereas more narrow sections are confined by minor, less resistant, Eocene aged formations. High channel-floodplain connectivity (CFC) is characteristic of this zone as a result of several paleo channels. The channels indicate movement within the valley; more than in other zones. Figure 8 provides a map of the zone.

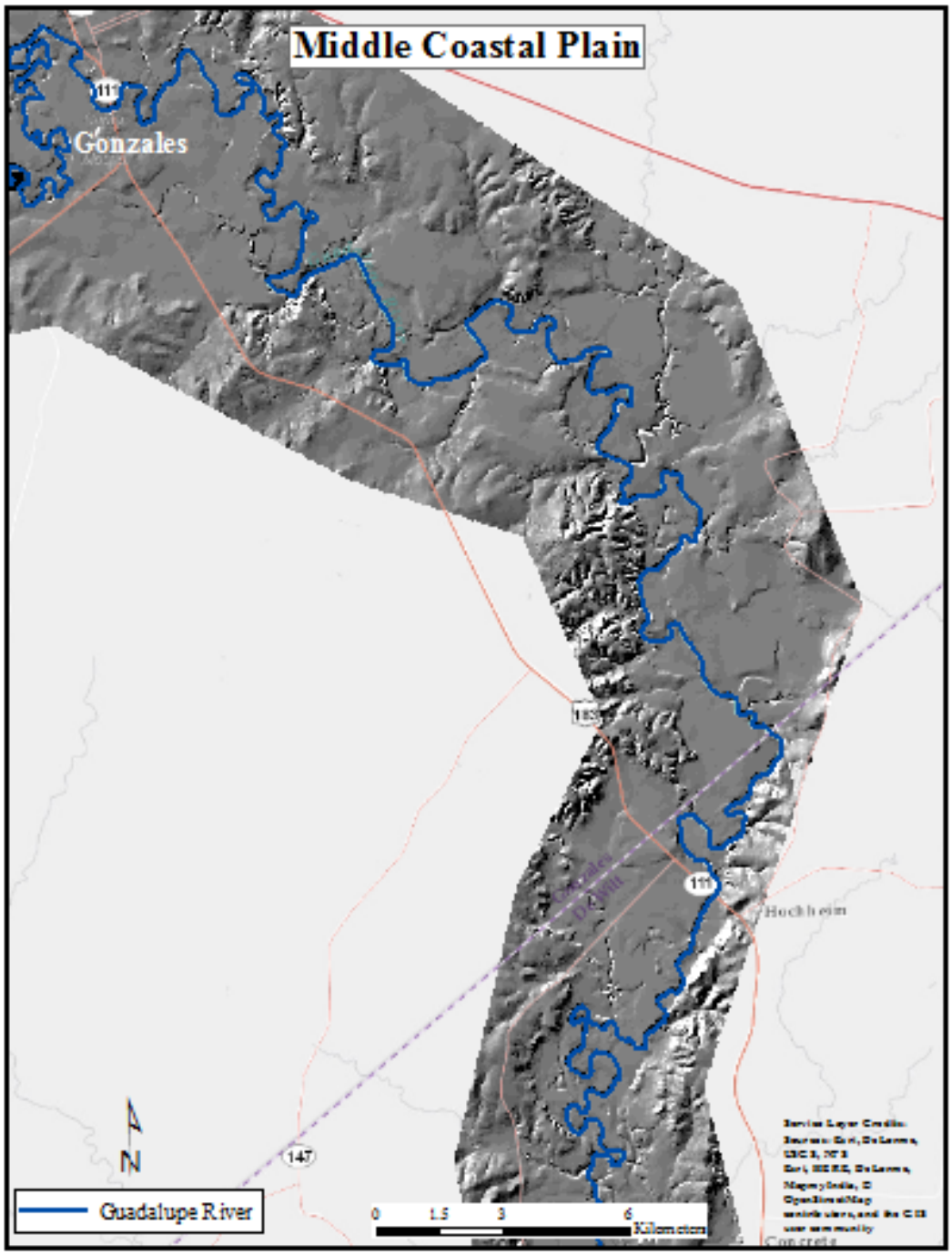


**(a)**

**Figure 8. Map of the Middle Coastal Plain geomorphic zone and sub-reach where (a) is the upper part of the zone and (b) is the lower part.**

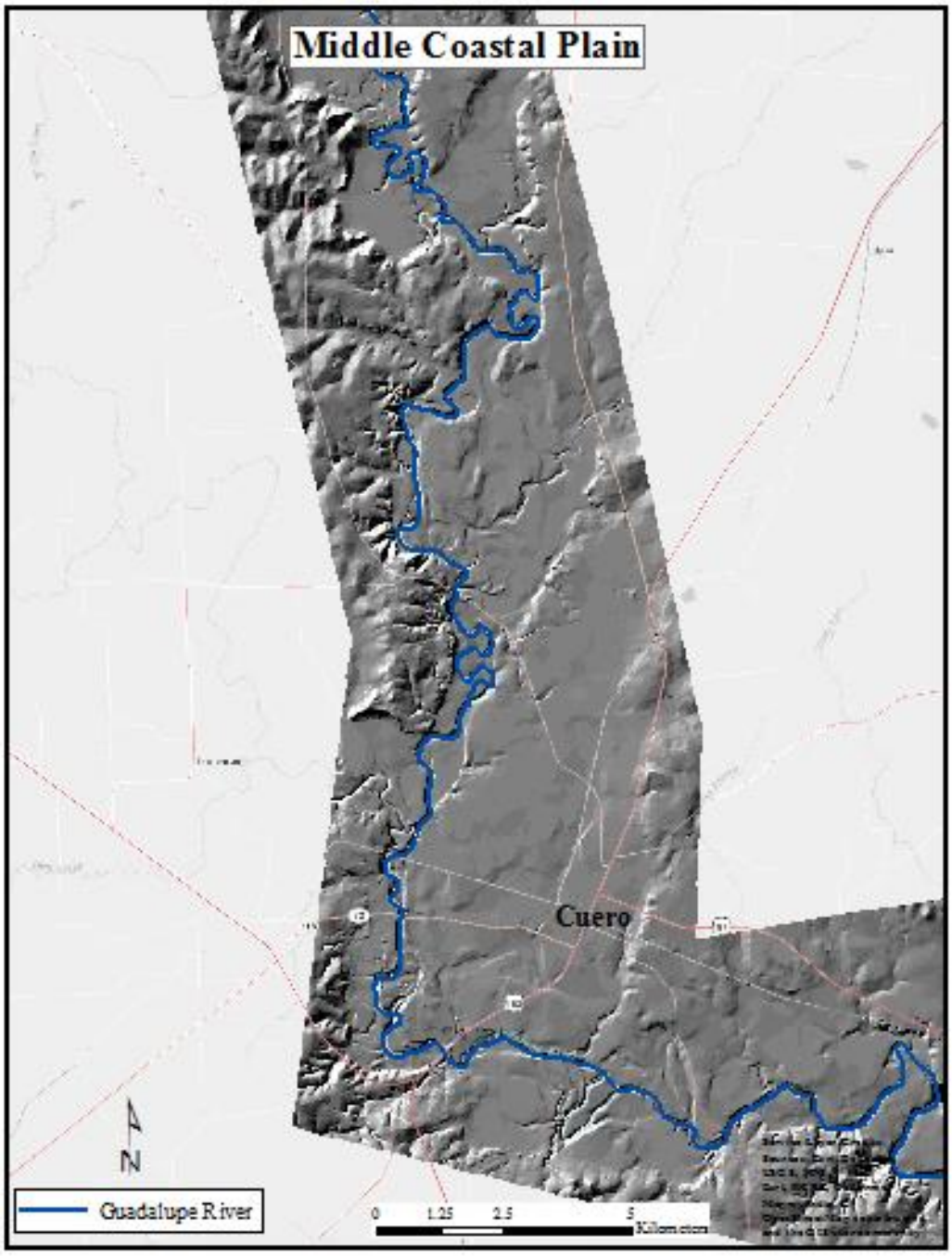


**(b)**

**Figure 8. Continued.**

### 3.1.4 Zone 4 – Coastal Plain Transition (CPT)

Zone 4 transitions from Miocene-aged valley walls near Cuero, TX to Pliocene-aged upstream of Victoria, TX. The 51 km reach decreases in sinuosity and has a low slope. Figure 9 provides a map of the zone.

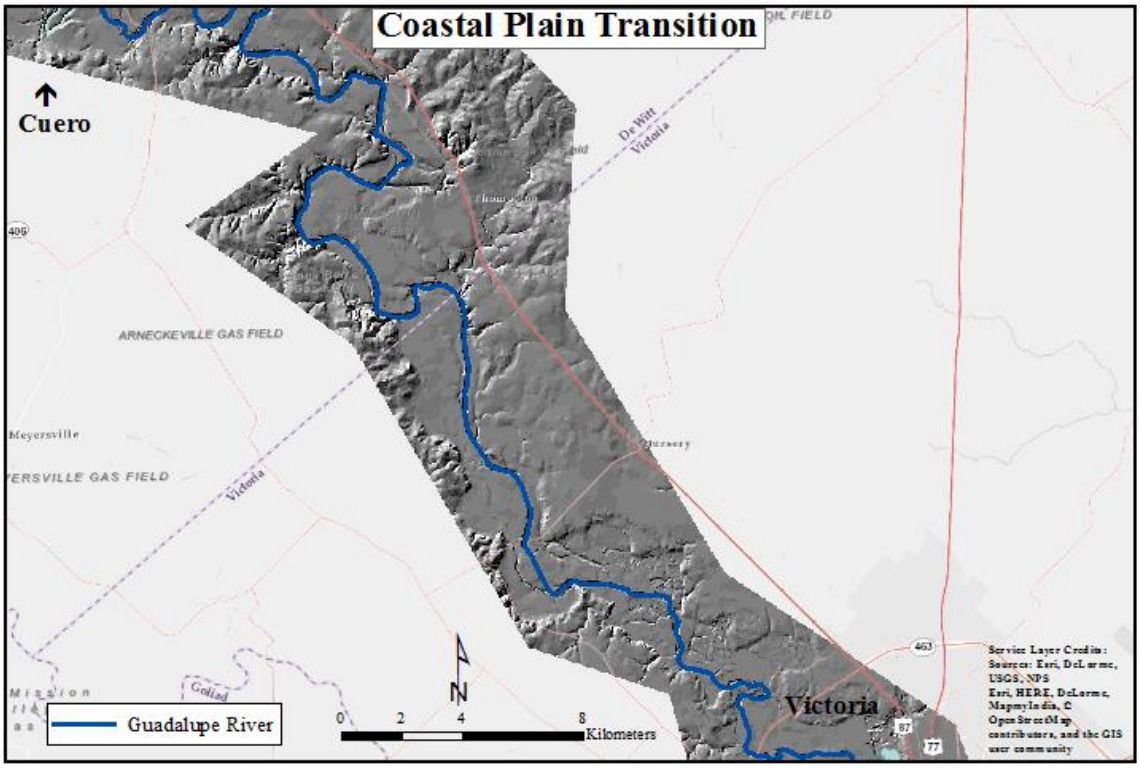


**Figure 9. Map of the Coastal Plain Transition geomorphic zone and sub-reach.**

### 3.1.5 Zone 5 – Lower Coastal Plain (LCP)

The lower coastal plain extends 39 km from upstream of Victoria, TX to zone 6. The reach has low slope, but is sinuous with a sinuosity less than two. Zone 5 has high

CFC as a result of low banks allowing for common overbank flow. Figure 10 provides a map of the zone.

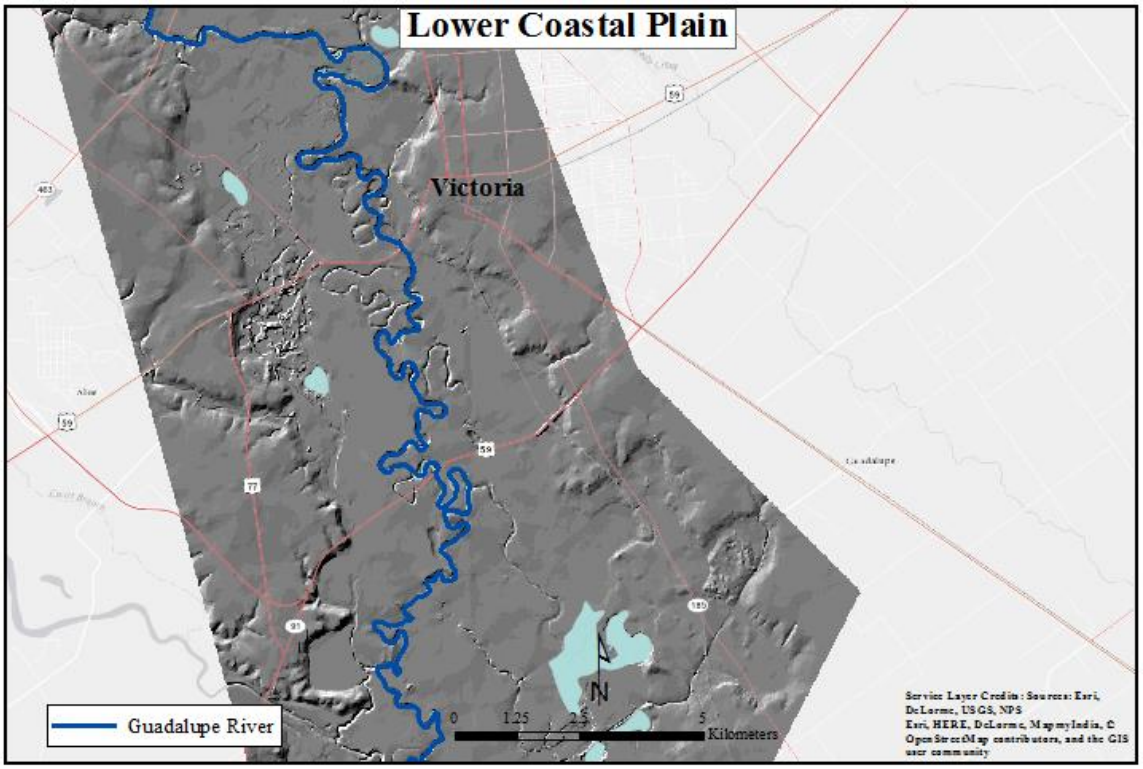


**Figure 10. Map of the Lower Coastal Plain geomorphic zone and sub-reach.**

### 3.1.6 Zone 6 – Upper Delta (UD)

The upper delta is a 25 km reach extending from the confluence with Coleto Creek to zone 7. Characteristic of a deltaic area, slope and sinuosity are low. The zone is far enough upstream from Guadalupe Bay, so is not affected by tides or backwater effects. An unconfined valley and low banks allow for very high CFC. Although

unconfined, cohesive Beaumont clays exhibit some control on channel morphology. Figure 11 provides a map of the zone.

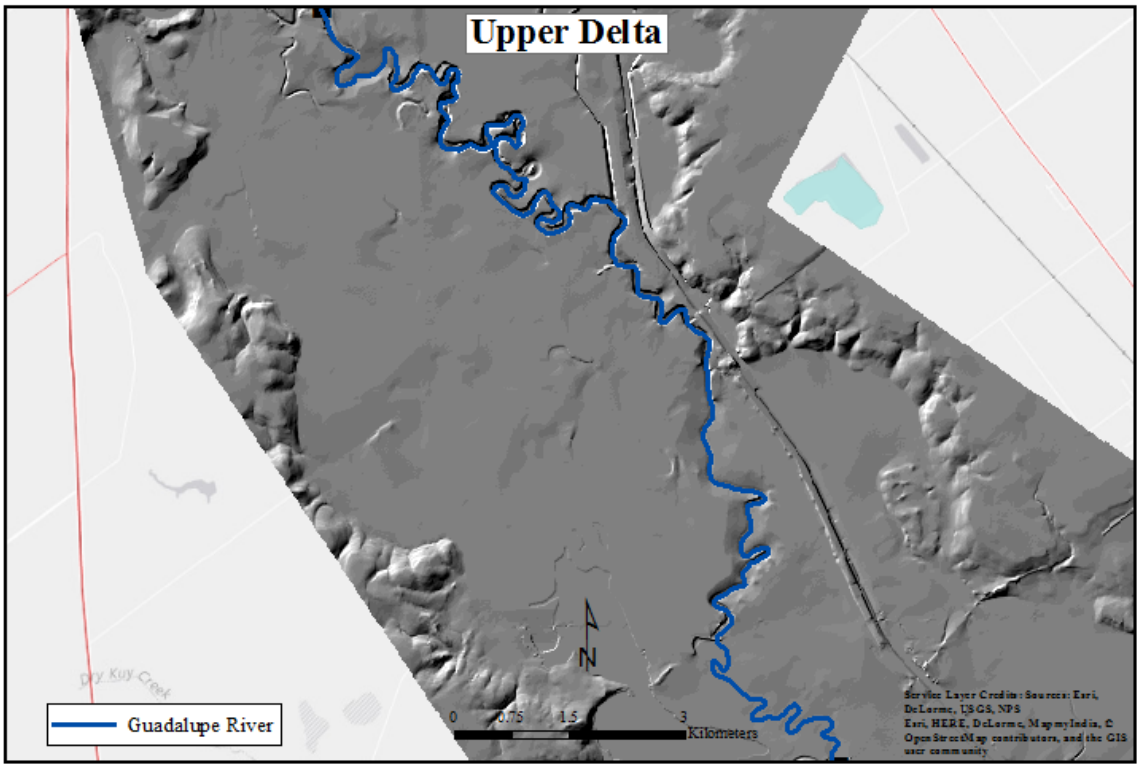


**Figure 11. Map of the Upper Delta geomorphic zone and sub-reach.**

### 3.1.7 Zone 7 – Middle Delta (MD)

The middle delta is a 23 km reach near Bloomington to just below the confluence with the San Antonio River. The zone is similar to the upper delta, but is more influenced by Guadalupe Bay. A saltwater barrier at Tivoli limits the amount of tidal and saltwater influence in the zone, but is present. Figure 12 provides a map of the zone.

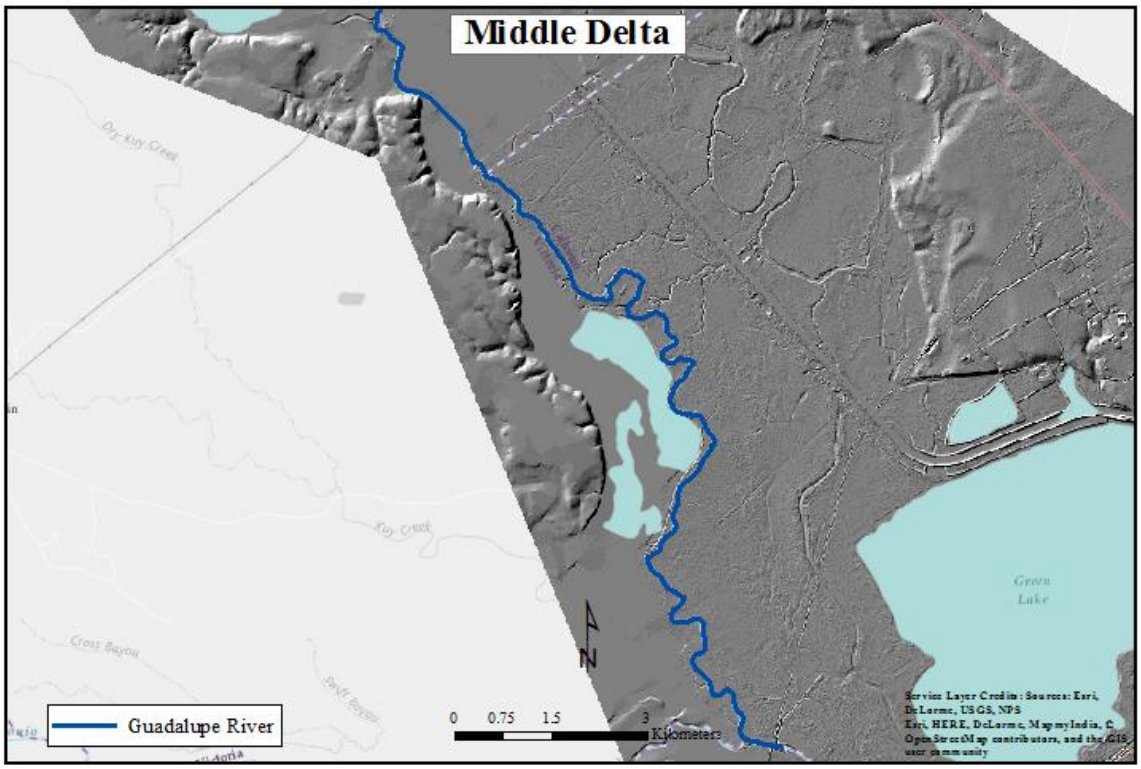


**Figure 12. Map of the Middle Delta geomorphic zone and sub-reach.**

*3.2 Geology and Geomorphology*

Included in the Guadalupe River basin is the Balcones Escarpment fault zone that acts as the divide between the uplifted Edwards Plateau and the Gulf Coastal Plain (Baker, 1976). The escarpment provides a natural divide between the contrasting upper and lower Guadalupe River. In the upper reach, the Edwards Plateau is a karst-dominated region made up of limestone, dolomite, and marl. Numerous confined, incised channels dissect the Plateau before flowing down the escarpment to the alluvial plain toward the lower reach. Here, the Gulf Coastal Plain is dominated by sand, silt and

clay. The lower river reach, of which this study encompasses, meanders across the largely unconfined alluvium toward the Gulf of Mexico.

Roughly 200 million years ago, the Guadalupe River Basin and much of Texas was under the sea. Figure 13 shows beds situated parallel to the current Gulf Coast as a result of sea regression.

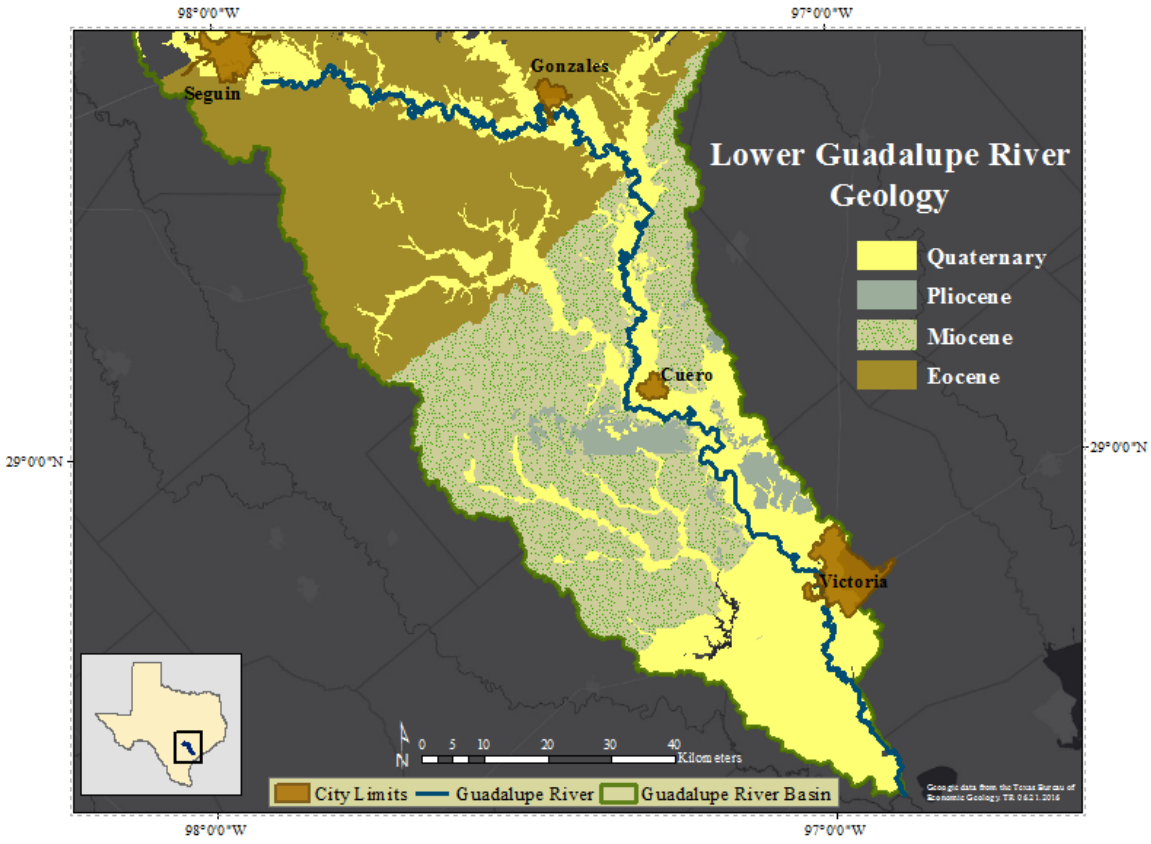


**Figure 13. Geology by age of the Guadalupe River Basin with study reach highlighted.**

Seguin to just east of Gonzales consists of the Eocene aged Wilcox Group, Recklaw, Yegua, and Manning Formations; all sand dominated. East of Gonzales, the Miocene aged Catahoula and Fleming Formation dominate until Cuero where the Pliocene clay and mud dominated sandstone of the Goliad and Willis Formation cut into the sand and mudstone Miocene formations. North of Victoria, the Pleistocene aged Lissie Formation dominated the western side of the river valley, whereas the Beaumont Formation dominates the east. The Lissie is sand-silt dominated whereas the Beaumont is predominately clay. Quaternary alluvium and terrace deposits dominate the valley as the river flows toward the Gulf (Deussen, 1924; Solis and Raul, 1981).

*3.3 Climate*

The climate of this region is considered subtropical humid, characterized by warm summers, and mild, dry winters. The average annual temperature is 19°C at the top of the reach in New Braunfels, 22 km northwest of Seguin. The hottest month is August where the average high is 35°C and low is 22°C. January is the coolest month where the average high is 16 °C and the low is 3°C. At the lower end of the reach, the mean temperature in Victoria is 21°C. The hottest month is August with an average high temperature of 35°C and low of 23°C. The coldest month is January with an average high of 18°C and a low of 6°C (USClimate Data, 2016).

Annual precipitation averages from 863 mm to 1047 mm in New Braunfels and Victoria, respectively. The majority of this falls as rain, and is heaviest in the spring, early summer, and fall. This region is unique because it experiences a variety of types of

storms capable of catastrophic rainfall. In the spring and early summer, cold fronts from the northwest meet moist air masses originating from the Gulf to create squall lines of thunderstorms that produce the majority of rainfall. In the fall, tropical disturbances and remnants will move landward, stalling out over the escarpment region with the potential to produce large amounts of rainfall.

*3.4 Land Use*

Table 3 below shows land use for the Guadalupe River watershed for 1992 and 2011. Percent change that has occurred over 19 years is also presented.

**Table 3. Land use/land cover for 1992 and 2011 and associated changes.**

| Land Unit | 1992 Land Cover Percentage | 2011 Land Cover Percentage | Percent Change (1992-2011) |
|---|---|---|---|
| **Open Water** | <1% | <1% | <1% |
| **Urban** | 1.8% | 8.6% | 6.8% |
| **Barren Land** | <1% | <1% | <1% |
| **Deciduous Forest** | 15.1% | 7.0% | -8.1% |
| **Evergreen Forest** | 20.2% | 10.5% | -9.7% |
| **Mixed Forest** | <1% | <1% | <1% |
| **Shrub/Scrub** | 16.7% | 36.3% | 19.6% |
| **Grassland/Herbaceous** | 22.6% | 8.2% | -14.4% |
| **Pasture/Hay** | 15.9% | 18.6% | 2.7% |
| **Cultivated Crops** | 5.6% | 6.2% | 0.6% |
| **Woody Wetlands** | <1% | 2.4% | 2.1% |
| **Emergent Herbaceous Wetlands** | <1% | <1% | <1% |

Overall, the watershed is predominantly shrub/scrub and pasture which accounts for about 55% of the land cover. Land use in the region has shifted from grasslands to

more pasture and scrub. Forested areas are scattered throughout the watershed, but are dominant along riparian areas. Urban presence and growth is minimal in the study area. Victoria is the largest urban area inside the watershed with a population of ~66,000 whereas Seguin has a population ~ 26,500 (Census.gov, 2014).

### *3.5 Vegetation*

The Guadalupe River cuts through four distinct vegetation regions including the Blackland Prairie which consists of abundant scrub and cultivated plots, Oak-hickory consisting of grasslands and stands of timber, and Fayette and Coastal Prairie hosting a majority of grasslands (Hatch et al., 1990).

Riparian cover changes throughout the watershed. The uppermost reaches of the Guadalupe are dominated by deciduous forest and cropland. Deciduous plants include cypress, oaks, and cottonwoods, but progressing down-river deciduous and croplands intersperse between the dominant grasslands.

# 4. METHODS

## *4.1 Total Rates of Migration*

To accomplish the objective of determining lateral rates of migration, a GIS was used. Imagery and historical maps were collected, georeferenced, and digitized for the years: 1951-1964 (as one group denoted as 1960 in the GIS), 1995, 2004, 2010, and 2014. Images for the period 1951-1964 are grouped as a result of various dates for USGS topographic maps. The images for 1960 were georeferenced to the 2004 imagery because it was pre-referenced and provided the highest quality resolution. All images and data were referenced using the projected coordinate system NAD 1983: UTM Zone 14 N. Table 4 includes the years and sources of imagery because each were acquired from various sources and have different spatial resolutions. Table 5 includes each study period and span of years for the period.

**Table 4. Collected imagery date and spatial resolution.**

| Study Period | Imagery Source (resolution) |
|---|---|
| **1960** | USGS Topographic Maps (~2.5m) |
| **1995** | Digital Ortho Quadrangles (~1m) |
| **2004** | National Agriculture Imagery Program (NAIP) (~1m) |
| **2010** | NAIP (~1m) |
| **2014** | NAIP (~1m) |

**Table 5. Study periods.**

| Study Years | Time Interval (Years) |
|---|---|
| **1960-1995** | 35 |
| **1995-2004** | 9 |
| **2004-2010** | 6 |
| **2010-2014** | 4 |

Each acquired image for the study year was combined into a mosaic in ArcGIS® to include the entire reach in the study period. River position was digitized at a scale of 1: 4,000 for all images. Spatial resolution ranged from 1-2 m for all images, so a scale of 1: 4,000 was seen as acceptable for the range of resolution. This scale was used for all images to minimize error and subjection resulting from one digitizer.

Other rules for digitization were also determined to streamline the process and reduce error. Banks were digitized using the edge of vegetation on an exposed channel bank to account for high and low flow periods (Richard et al., 2005). For exposed point bars, the established vegetation line was used to delineate the boundary. In areas where dense vegetation covered the channel boundary, bank lines were drawn through the canopy (Winterbottom, 2000).

From the digitized left and right banks of the river, a centerline was created using the "collapse dual lines to centerline" tool in ArcGIS®. The centerline does not represent the thalweg, but rather the exact center between the bank lines. A central line provides a clear representation of lateral rates of migration, and minimizes error from digitization.

It also eliminates bias of thalweg position not necessarily changing when channel boundaries do.

Centerlines are compared using the “feature to polygon” tool in ArcGIS®. Polygons are created between centerlines time 1 and time 2. Figure 14 displays single polygons created.

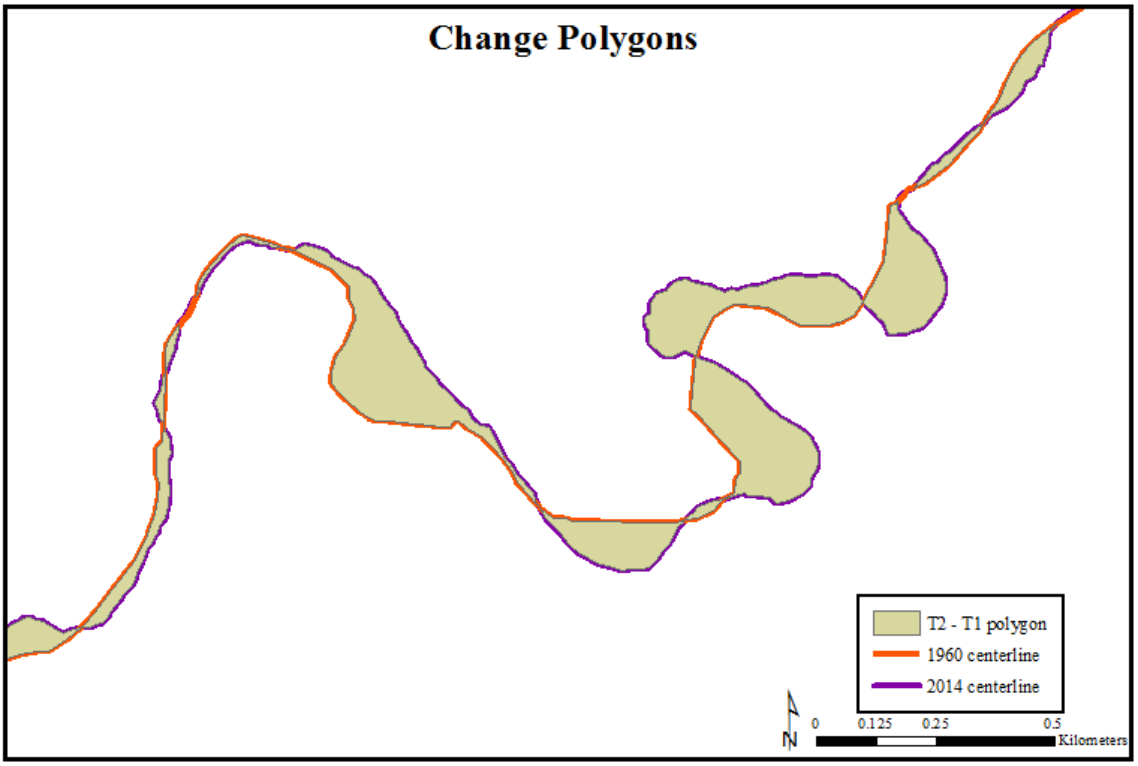


**Figure 14. Map showing change polygons created from subtracting time 2 (T2) from time 1 (T1) centerlines to generate a polygon of change in area.**

Figure 15 shows an example of consecutive meander bends with stacked polygons for each interval. The stacked polygons display the progression of lateral migration over the study period.

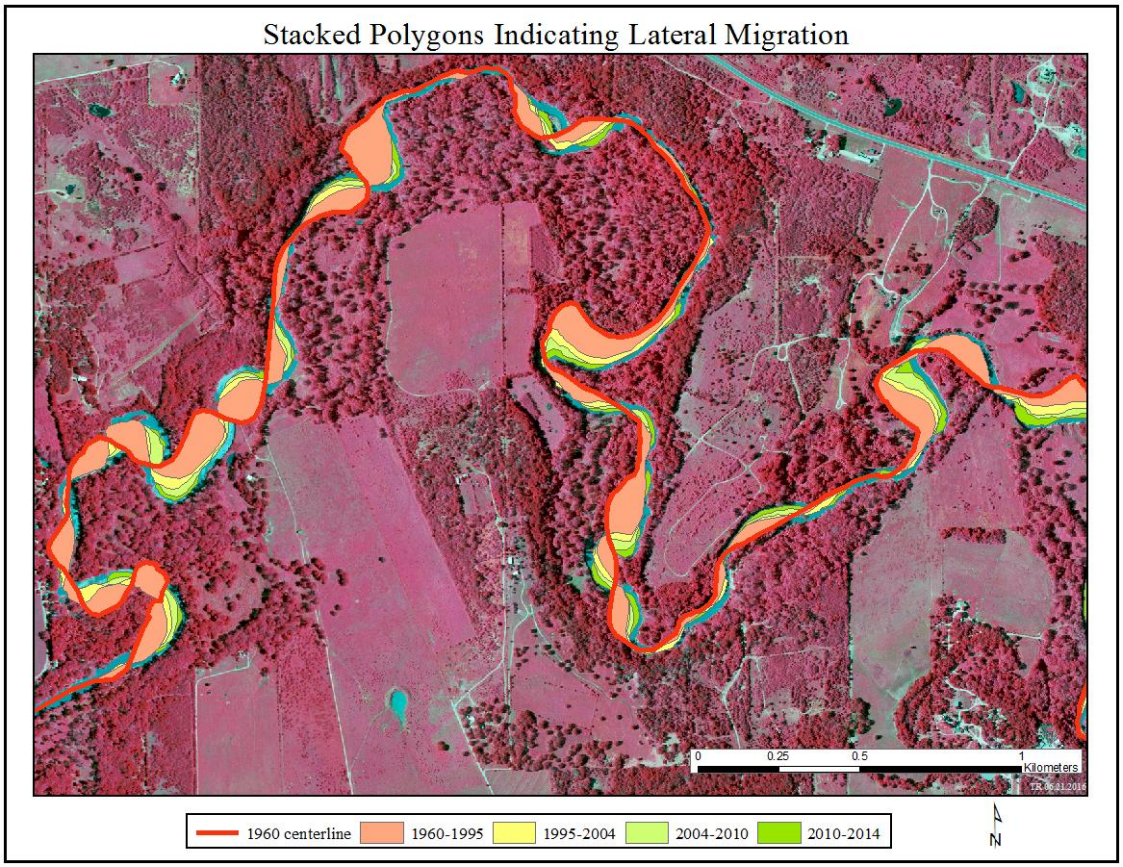


**Figure 15. Map showing stacked polygons created from centerline pairs.**

From the polygons, total amounts of migration between time intervals were calculated. Total migration is calculated as follows:

$$M_n = \frac{A}{\frac{1}{2}P} \quad \text{(Eq. 2)}$$

where $M_n$ is the total rate of migration, $A$ is the area of the polygon, and $P$ is the perimeter of the polygon. From the total amount, yearly rates are calculated as follows:

$$R_y = \frac{M_n}{N} \quad \text{(Eq. 3)}$$

where $R_y$ is the yearly rate, $M_n$ is the total rate of migration, and $N$ is the number of years in the study period. To minimize spatial error associated with digitizing and using imagery of various resolutions, total migration amounts less than 6 m were eliminated. Table 6 lists the number of polygons created for each time interval.

**Table 6. Number of polygons with an amount greater than 6 m total migration.**

| Study Years | Number of Polygons |
|---|---|
| **1960-1995** | 651 |
| **1995-2004** | 411 |
| **2004-2010** | 247 |
| **2010-2014** | 251 |
| **1960-2014** | 745 |

Change polygons do not distinguish between positive and negative migration. This study does not distinguish that because any movement, positive (erosion) or negative (aggradation) is a result of instability. The purpose of this study is to determine

the stability of the lower Guadalupe River, so instability of any kind is used as an indicator.

*4.2 Geomorphic Zones and Specific Meander Bends*

To determine the driving mechanisms associated with lateral migration, an analysis was completed separating the reach into the seven sub-reaches based on geomorphic zones. The zonal boundaries were imported into ArcGIS® following the work of Phillips (2011). The upper and lower zones are adjusted to encompass the top and bottom end of this study reach. Polygons calculated for the entire reach were sectioned and divided into the seven sub-reaches.

To further understand the sub-reaches, meander bends were chosen at random for further analysis. Not all meander bends in the study reach were assessed as a result of the high number of bends. The "create random points" tool was used to generate ten points per sub-reach. A 2 km buffer was used to eliminate potential clustering in one bend. If a point was generated between two bends, the closer bend was chosen to be analyzed. The total time period 1960 – 2014 was used for analysis. Initially, each time period, four in total, were assessed for the first and fourth sub-reach. No significant change in radius of curvature measurements were detected, so it was determined that total time period would be sufficient for analysis. A total of 70 meander bends were analyzed for the time period for a total of 140 points.

Channel characteristics, including type of bend (compound or simple), radius of curvature, channel width, slope, and sinuosity, were calculated for each point.

Watershed characteristics, including riparian presence, density, and bank composition, were also collected.

### 4.2.1 Radius of Curvature

To determine radius of curvature, I used a method adapted from Nanson and Hickin (1983) by Geist (2005). Two separate circles are fit to the bend where the radii from the two circles are averaged, and the result is the radius of curvature. To determine the best fit for two circles, the point of maximum curvature of the specific bend must be determined from the original channel placement. 1960 and 2014 were used in the analysis, so the 1960 outer channel boundary was used as the reference. The Guadalupe River has a series of compound bends, or bends embedded within a larger bend, thus, it is challenging to distinguish which bend and associated point of maximum curvature to choose. Figure 16 from Brice (1974) displays a variety of shapes of meander bends and was, thus, used as a reference to choose the appropriate bend and maximum point of curvature.

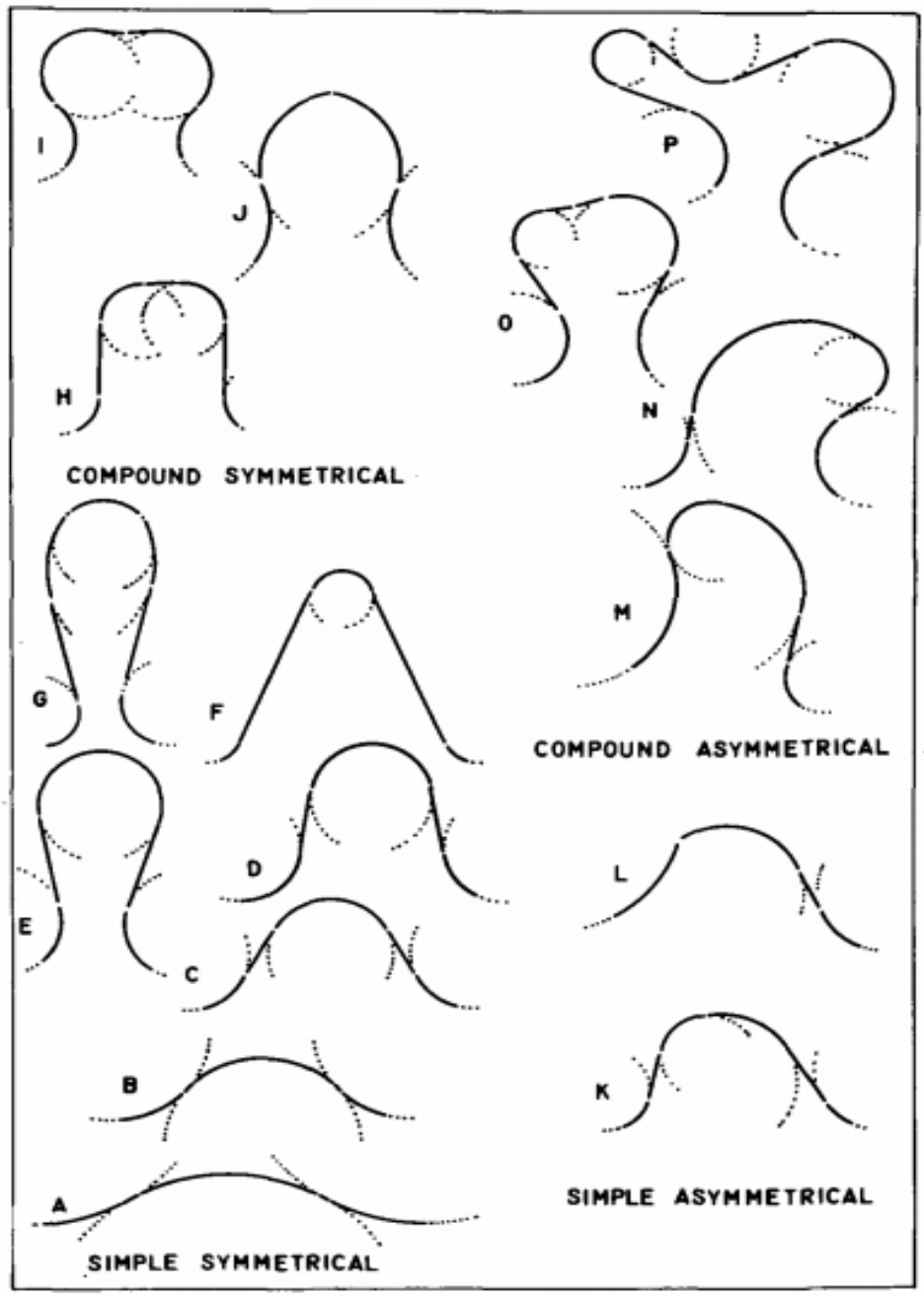


**Figure 16. Types of meander bends. Flow is right to left. (Modified from Brice, 1974).**

Once the appropriate bend and maximum point of curvature are determined, five points of channel width are measured within the meander bend, between both points of inflection, and an average width is found. Points of inflection determine one meander bend from another, so it is important to keep measurements between these two points. The average width is then used as the arc length spacing to place two points on either side of the maximum point of curvature. The first circle is fit to the three innermost points and the outer is fit to the middle point and two outer points. Figure 17 shows an example of a measurement of the radius of curvature in meander bend for 1960.

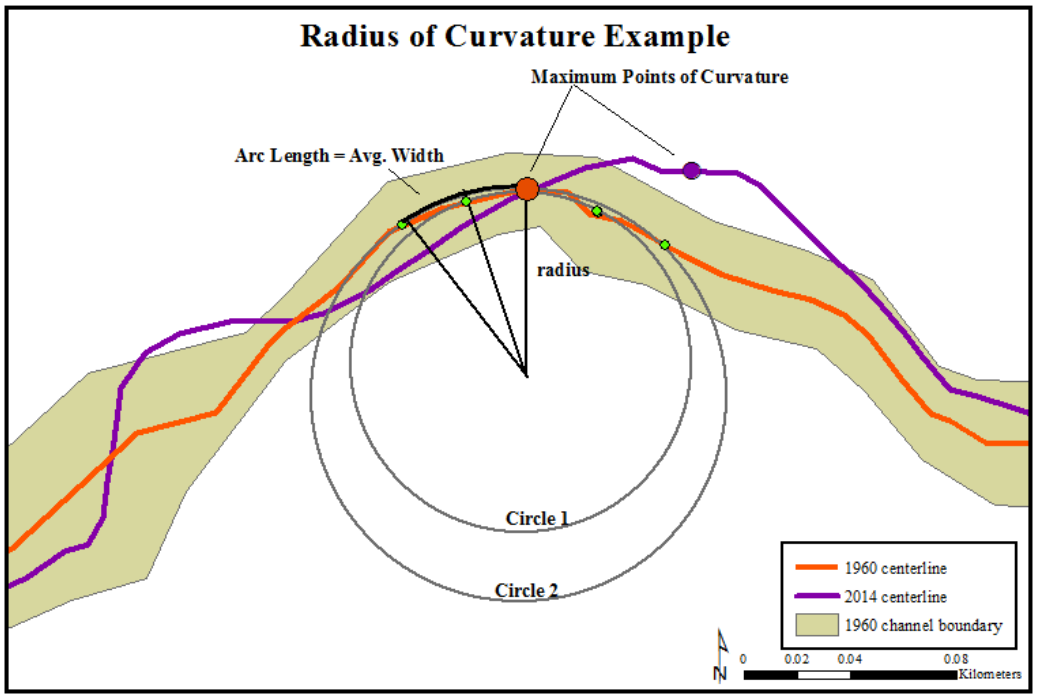


**Figure 17. Radius of curvature example using 1960 channel boundary.**

### 4.2.2 Slope and Sinuosity

After measuring the radius of curvature, local slope was determined for each bend using a 2014 10 m digital elevation model (DEM). Slope was assumed constant through time. Points of measurement were generated at 1 km intervals for the study reach. Slope was determined using the elevation difference between points that were 2 km apart to encompass the entire bend. Local sinuosity was also measured using the same points for consistency. Channel length was divided by valley length between the 2 km spaced points to determine sinuosity.

### 4.2.3 Vegetation

Channel planform variables were measured along with channel characteristics including vegetation and bank composition. The presence of vegetation was determined from 2014 imagery for each bend on the inside and outside boundaries. A 500 m buffer was used on both banks to be sure to encompass the entire floodplain. The buffer was also used for land use/land cover categories. Inside and outside land cover were noted for each bend as either forest (tree vegetation), barren (scrub, grasslands, cropland, road), or wetlands.

Composition of inside and outside channel banks were determined from the Natural Resources Conservation Service (NRCS) shapefiles of county soil surveys. A shapefile and associated database were used in a GIS to determine bank composition. Assumptions were made that cut banks along the outside bend are homogenous to the

surface as a result of surficial mapping only. The same 500 m buffer was used to determine dominant soil type, silt-clay percentage, and soil hydrologic unit.

### 4.2.4 USGS Gauging Stations

To further determine mechanisms of lateral migration, the dynamics of discharge were assessed for the study reach. United States Geological Survey (USGS) gauging stations provide consecutive and continuous measurements of discharge at four sites within the reach. Figure 18 shows the location of the four gauging stations within the reach and Table 7 shows the variability of each stations period of record presented in order moving downstream.

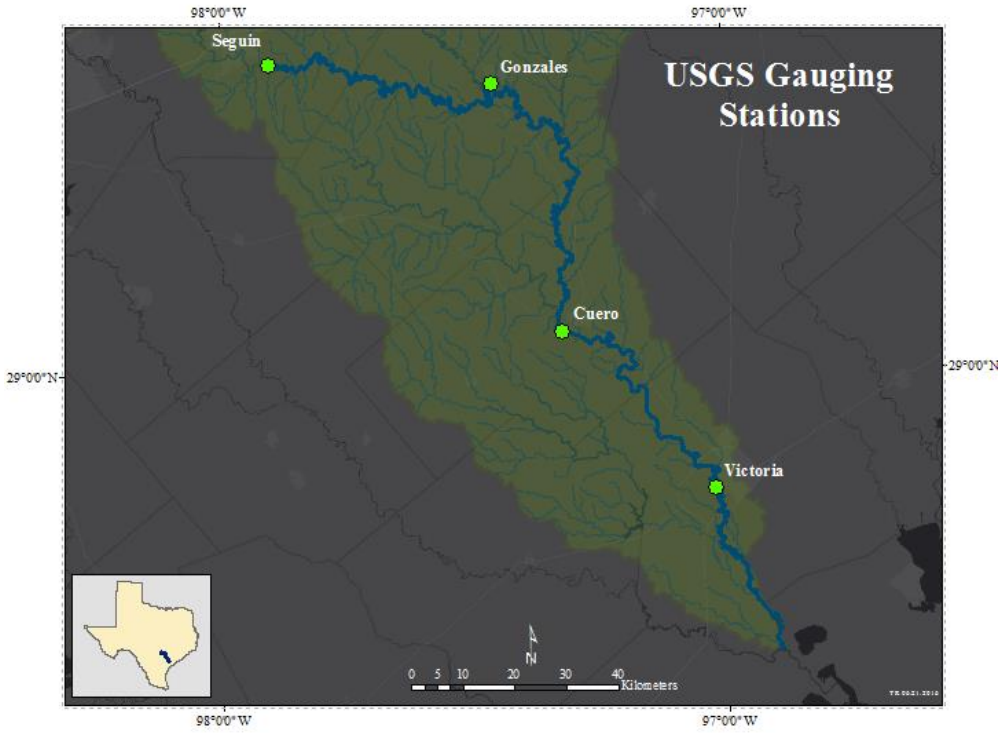


**Figure 18**. **USGS gauging station locations within the lower Guadalupe River reach.**

**Table 7. USGS gauging stations and period of record.**

| Guadalupe River near | Gauge ID | Gauge Discharge Record Start | Drainage Area ($km^2$) | Distance from Gulf (km) |
|---|---|---|---|---|
| **Seguin** | 08169792 | 3/15/2005 | 5069 | 399 |
| **Gonzales** | 08173900 | 10/12/1996 | 5617 | 282 |
| **Cuero** | 08175800 | 1/1/1964 | 7941 | 165 |
| **Victoria** | 08176500 | 11/4/1934 | 13463 | 68 |

A single gauging station near Victoria, TX was chosen for analysis as a result of geographic location at the end of the study reach and far enough from tidal influence of the Gulf of Mexico. The station also has the longest period of record of 81 years. Average monthly and annual discharge were calculated and used in analysis for each of the study periods.

Gauging stations also provide a means to obtain a rough estimate of stream power using Eq. (1). Each station was analyzed to find a five consecutive day time period with minimal variability of discharge between both stations. Stage height, at the determined time period, was added to the surveyed elevation of the gauge. Upstream elevation was subtracted from downstream elevation and divided by the channel length to obtain a value for slope of the water surface. The assumption is that slope is constant between gauging stations.

Average daily discharge was then calculated for each station and used in the stream power equation to obtain an average stream power for the reach. Bankfull stream power was also calculated using the stage and associated discharge when the river reaches bankfull, or minor flood stage as defined by the USGS and National Weather

Service (NWS). Initial reaches used to calculate stream power are defined by gauging station and not the geomorphic boundary sub-reach to obtain a more accurate value. Sub-reaches were analyzed using a calculated slope from the 10 m DEM and average discharge of the nearest gauging station.

*4.3 Statistical Analysis*

Once all variables are collected, analysis of variance (ANOVA) tests were used to identify possible mechanisms of lateral migration. All statistical analyses were performed with JMP® software. The dependent variable, total migration, was analyzed against collected independent variables for the entire reach and sub-reaches. For this analysis, it is assumed that all variables are independent of each other. Resulting F-statistic and p-values, indicating level of confidence, guided the analysis toward controlling variables.

# 5. RESULTS

## *5.1 Lateral Channel Migration – 380 km Reach*

Table 8 provides an overview of each time period for the entire study reach. Five time periods are provided, including the total time period.

**Table 8. Study time periods for entire study reach with associated migration polygons and average rates of migration.**

| Study Years (Span) | Number of Polygons | Minimum Migration (m) | Maximum Migration (m) | Average Total Migration (m) | Average Rate of Migration (m/yr) |
|---|---|---|---|---|---|
| **1960-1995 (35)** | 651 | 6.00 | 87.11 | 15.1 | 0.43 |
| **1995-2004 (9)** | 411 | 6.00 | 201.83 | 10.27 | 1.14 |
| **2004-2010 (6)** | 247 | 6.00 | 133.74 | 10.58 | 1.06 |
| **2010-2014 (4)** | 251 | 6.00 | 178.79 | 9.86 | 2.47 |
| **1960-2014 (54)** | 745 | 6.00 | 221.47 | 19.5 | 0.36 |

Although each time period has a different span, rates of migration are normalized by dividing total migration by number of years in the study period. This allows rates of migration to be compared in each study period without bias.

To further remove bias, the inclusion of avulsions, or meander cut-offs, in analysis was investigated. Avulsions have the potential to skew the data toward larger rates of migration, thus, it is important to pinpoint avulsions and account for them in the analysis. Results in Table 8 include avulsions. Table 9 provides the number of avulsions

in each time period, and the associated difference in migration and rate of migration with and without avulsions.

**Table 9. Avulsion occurrence and how it affects the total and rates of lateral migration.**

| Study Period | Number of avulsions | Average Rate of migration w/o avulsions | Average Rate of migration with avulsions | Average Total migration w/o avulsions | Average Total migration with avulsions |
|---|---|---|---|---|---|
| **1960-1995** | 1 | 0.43 | 0.43 | 14.93 | 15.10 |
| **1995-2004** | 4 | 1.01 | 1.14 | 9.13 | 10.27 |
| **2004-2010** | 2 | 0.95 | 1.06 | 9.47 | 10.58 |
| **2010-2014** | 0 | 2.30 | 2.47 | 9.19 | 9.86 |
| **1960-2014** | 7 | 0.34 | 0.36 | 18.15 | 19.50 |

After comparing the total migration and rates of migration with and without avulsions in the dataset, the change is minimal. Although a minimal change, analysis will proceed without avulsions. This will provide a less skewed average when smaller sub-reach datasets are analyzed.

To visualize results from the entire reach analysis, Figure 19 shows a boxplot of lateral rates of migration for each time period. Each point represents a migration polygon with total migration of 6m or more. Total migration is used as a general indicator, but rates of migration are used to normalize the data and compare across study time periods as rates are per year.

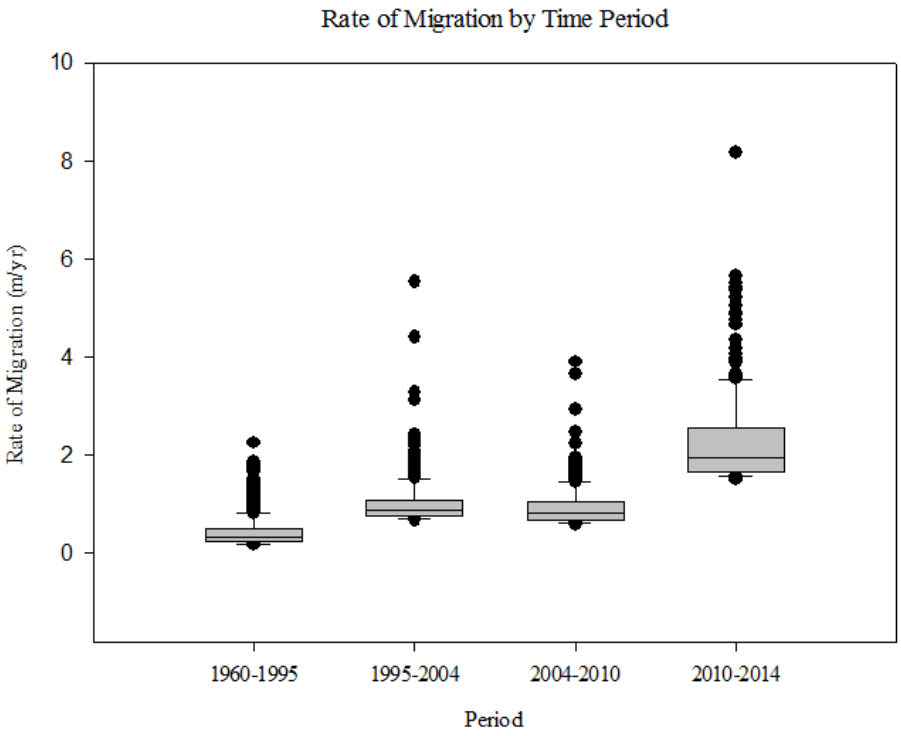


**Figure 19. Boxplots of points of lateral migration for each time period.**

Results show that variability in rates of migration increase from 1960 to 2014. The period 2010-2014 stands out as having the highest median rate of migration, while also having the highest minimum and maximum rate for all time periods.

*5.2 Discharge and Rates of Migration*

To understand the mechanisms controlling the variability of rates of migration for the study periods, discharge was related to rates of migration. Lateral migration has been established as a function of discharge (Gillespie and Giardino, 1997; Briaud, 2001; Hooke, 2003; Phillips, 2012). Discharge can be the main influence on lateral migration,

but it is often coupled with, or driving, other processes closely related to lateral migration. Therefore, the dynamics of the river and lateral rates of migration need to be understood as a result of discharge variability.

The USGS gauge near Victoria, TX was used for analysis for its geographic location and period of record. It was also determined that the gauge at Victoria is an appropriate analog for discharge variability along the lower Guadalupe River because of minimal variance between the gauges within the study reach. Figure 20 shows average monthly discharge for the period 1995-2015 to encompass the period of record for each gauge.

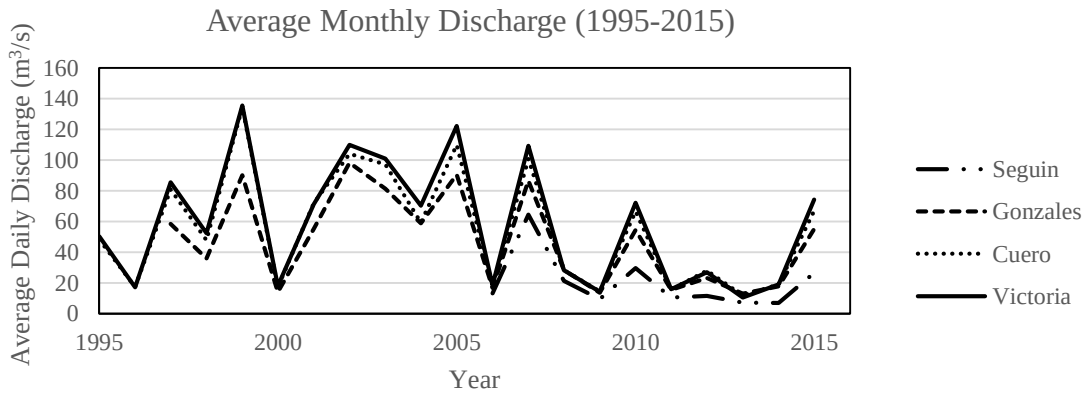


**Figure 20. Average monthly discharge for the period 1995-2015 for four gauges within the study reach.**

Discharge increases moving downstream and no major tributary inputs occur after the San Marcos River confluence in Gonzales until the San Antonio River confluence below Victoria. As a result, the Cuero gauge follows closely to Victoria.

Throughout the period of record for the Cuero gauge, the largest difference in monthly average between the two gauges is 97.69 $m^3/s$ in November 2004. Discrepancies arise during precipitation because runoff into the river is dependent on location and movement of the precipitation. This can affect discharge at one gauge and not another. Overall the variance is minimal, however, so the Victoria gauge is used for analysis. Figure 21a presents the average monthly discharge for the period of record at the Victoria gauge with associated average rates of migration for each study period. Figure 21b shows the average daily discharge and associates average rate of migration for each time period.

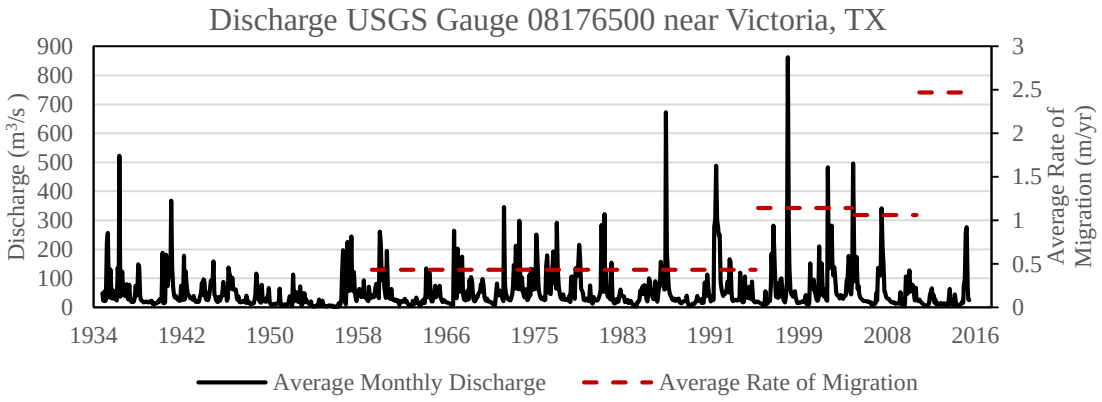


**(a)**

**Figure 21. (a) Average monthly discharge and average rates of migration per study time period. (b) Average daily discharge and average rates of migration per study time period.**

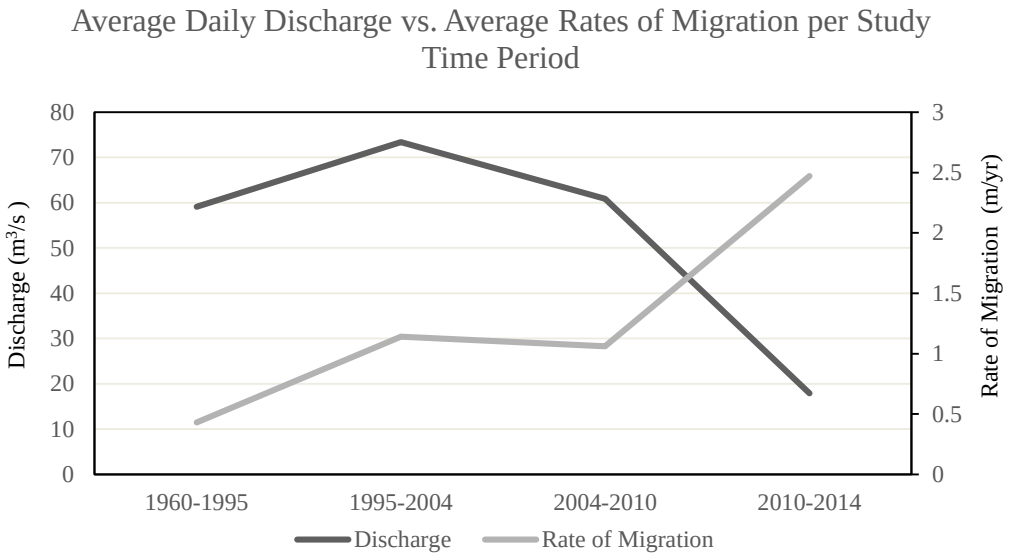


**(b)**

**Figure 21. Continued.**

Rate of migration and discharge follow a similar trend for the first three study periods, but conflict for the last period of 2010-2014. The lowest discharge has the highest average rate of migration. Observing the variability in flow regime in Figure 21a shows that no high-discharge months occurred during the time period as compared to the others.

To gain a better understanding of variance in flow regime for high-discharge months, daily average discharge was analyzed for each study period to pinpoint floods. It is known that one event can significantly alter a channel, however, this does not seem to be the case for the lower Guadalupe. Table 10 shows the study period and associated

number of events at flood stage. Moderate flood stage at the USGS gauge near Victoria was used. Moderate flood stage is 9m and discharge is ~990 $m^3/s$ (Nws.gov, 2016).

**Table 10. Study period and associated flood stage events.**

| Study period | Number of flood-stage events |
|---|---|
| **1960-1995** | 10 |
| **1995-2004** | 4 |
| **2004-2010** | 1 |
| **2010-2014** | 0 |

Ten major floods occurred during the 1960-1995 and the period of 1995-2004 had floods every other year including two record-setting events. Rates of migration however, are lower than the 2010-2014 period with no major events. The period 2010-2014 experienced a major drought that may have related to rates of migration for the time period.

*5.3 Stream Power and Rates of Migration*

Although flooding, with high stream powers, and rates of migration have minimal association, the relationship between stream power and rates of migration is investigated. Stream power was calculated for four reaches within the study reach as a result of gauge-station locations. Table 11 provides average stream power and average bankfull stream power for each reach. Bankfull stream power is based on the discharge at minor flood stage for each gauge. Values were calculated with the assumption that

slope and average discharge are constant throughout a reach and through time. Stream power is presented in watts per meter.

**Table 11. Stream power for each gauging station. $Q_{\mu}$ = average discharge.**

| USGS Gauging Station | Study Period | Slope | $Q_{\mu}$ ($m^3/s$) | Stream Power ($Q_{\mu}$) (W/m) | Bankfull Stream Power ($Q_{\mu}$) (W/m) |
|---|---|---|---|---|---|
| **Seguin** | 1960-1995 | 0.000443 | - | - | - |
| | 1995-2004 | | - | - | - |
| | 2004-2010 | | 27.96 | 121.53 | 2400.34 |
| | 2010-2014 | | 9.13 | 39.71 | 2400.34 |
| **Gonzales** | 1960-1995 | 0.000297 | - | - | - |
| | 1995-2004 | | 61.77 | 180.20 | 1163.93 |
| | 2004-2010 | | 48.43 | 141.30 | 1163.93 |
| | 2010-2014 | | 17.49 | 51.04 | 1163.93 |
| **Cuero** | 1960-1995 | 0.000344 | 55.92 | 188.62 | 1331.78 |
| | 1995-2004 | | 70.03 | 236.23 | 1331.78 |
| | 2004-2010 | | 62.94 | 212.33 | 1331.78 |
| | 2010-2014 | | 22.29 | 75.18 | 1331.78 |
| **Victoria** | 1960-1995 | 0.000148 | 58.85 | 85.48 | 374.73 |
| | 1995-2004 | | 73.47 | 106.73 | 374.73 |
| | 2004-2010 | | 60.85 | 88.39 | 374.73 |
| | 2010-2014 | | 18.18 | 26.40 | 374.73 |

As a result of lack of data for all gauging stations and the 2011-2012 drought, average stream power is compared using the data from 2004-2010. The reach between Cuero and Victoria has the highest value at 212.33 W/m, whereas the reach from Seguin to Gonzales has the highest average bankfull stream power value at 2400.34 W/m.

Stream power was also calculated using slopes determined from a 10m DEM for each sub-reach. The gauging station closest to the sub-reach is used for average daily discharge. Figure 22 compares average stream power to the longitudinal river profile.

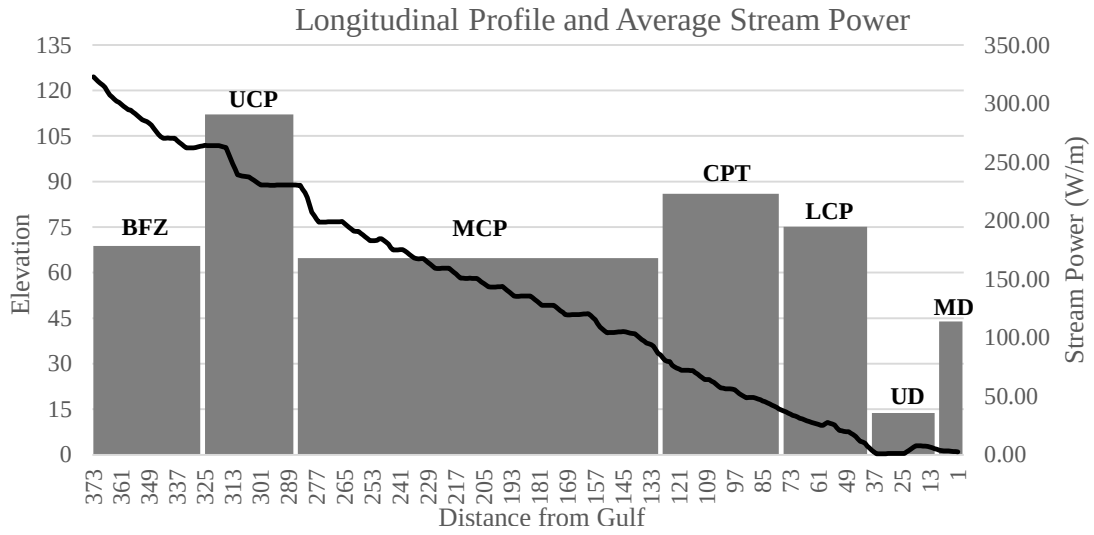


**Figure 22. Longitudinal profile of lower Guadalupe River study reach with average stream power for each sub-reach reach.**

The UCP reach has the highest average stream power at 290.67 W/m. The reach includes a knickpoint, or sudden change in slope, as a result from the dam that exaggerates values for slope and stream power. The CPT has the second highest average stream power at 222.78 W/m. The lowest average stream power of 35.7 W/m is in the UD reach where subsidence is occurring.

Table 12 compares average stream power to average rates of migration for the 2004-2010 study period.

**Table 12. Average rate of migration vs. average stream power.**

| Geomorphic Zone | Average Rate of Migration (2004-2010) (m/yr) | Average Stream Power (2004-2010) (W/m) |
|---|---|---|
| **Belmont Fault Zone** | 1.05 | 178.31 |
| **Upper Coastal Plain** | 0.93 | 290.67 |
| **Middle Coastal Plain** | 0.89 | 167.89 |
| **Coastal Plain Transition** | 0.96 | 222.78 |
| **Lower Coastal Plain** | 0.96 | 194.84 |
| **Upper Delta** | 0.83 | 35.70 |
| **Middle Delta** | 0.65 | 113.96 |

A relationship is lacking between average rates of migration and average stream power for each sub-reach. This may be the result of significantly generalizing the values of stream power. Assumptions have been made, and geometric factors including channel roughness and width-depth ratio, as well as the influence of sediment are not accounted for. A more in-depth analysis and accurate interpretation of stream power for each sub-reach could yield a more distinct relationship between the two variables.

*5.4 Lateral Channel Migration – Sub-Reaches*

Lateral rates of migration were analyzed at a sub-reach scale to gain a clear understanding of lateral migration along the lower Guadalupe River as well as to better

determine the mechanisms influencing channel migration. Rates of migration were calculated for each study period within each sub-reach. Figure 23 displays the trend of rates of migration moving downstream by geomorphic zone and provides the average rate of migration for each zone for the full study period.

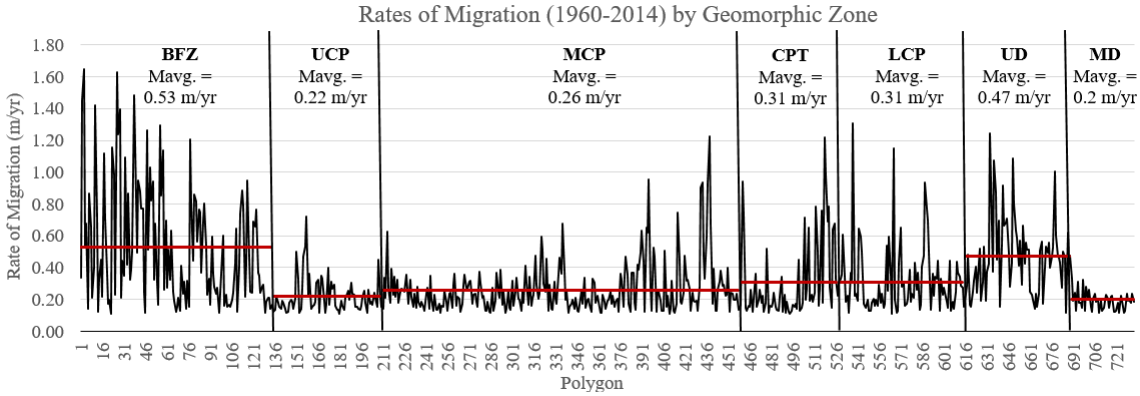


**Figure 23. Lateral rates of migration by zone. The x-axis represents each migration polygon; 1 is the uppermost reach while 721 is the downstream end. Geomorphic zone and associated average rate of migration are provided (red line).**

Sub-reach rates of migration were also analyzed for each time period. Table 13 provides the average rates of migration for each time period and Figure 24 provides a visual of the data.

**Table 13. Average rates of migration in meters per year by geomorphic zone for each study period.**

| | Average Rates of Migration (m/yr) by Geomorphic Zone | | | | | | |
|---|---|---|---|---|---|---|---|
| **Study Period** | BFZ | UCP | MCP | CPT | LCP | UD | MD |
| **1960-1995** | 0.61 | 0.35 | 0.34 | 0.34 | 0.36 | 0.67 | 0.25 |
| **1995-2004** | 1.22 | 0.92 | 0.98 | 1.03 | 1 | 0.83 | 0.74 |
| **2004-2010** | 1.05 | 0.93 | 0.89 | 0.96 | 0.96 | 0.83 | 0.65 |
| **2010-2014** | 2.51 | 2.49 | 2.05 | 2.34 | 2.19 | 1.77 | 1.54 |
| **1960-2014** | 0.53 | 0.22 | 0.26 | 0.31 | 0.31 | 0.47 | 0.20 |


**Figure 24. Graph of average rates of migration by study period for each geomorphic zone.**

Variability is seen between and within each zone for the full time period as well as the individual study periods. To obtain a better understanding of the variability and where migration is occurring, rates of migration were classified into three groups of low, medium, and high rates. Classes were designated using a natural breaks Jenks classification in ArcGIS®. Natural breaks were chosen as a result of the variability within each study period and a highly right-skewed dataset for each time period. Jenks' natural breaks partitions data by a goodness of variance fit measure. This method has been widely used for highly skewed data (Brewer and Pickle, 2002; Baz et al., 2009; Jiang, 2013).

Areas of highest rates of migration were calculated for each time period for the study reach. Figure 25 displays the maximum points of migration along the 380 km reach.

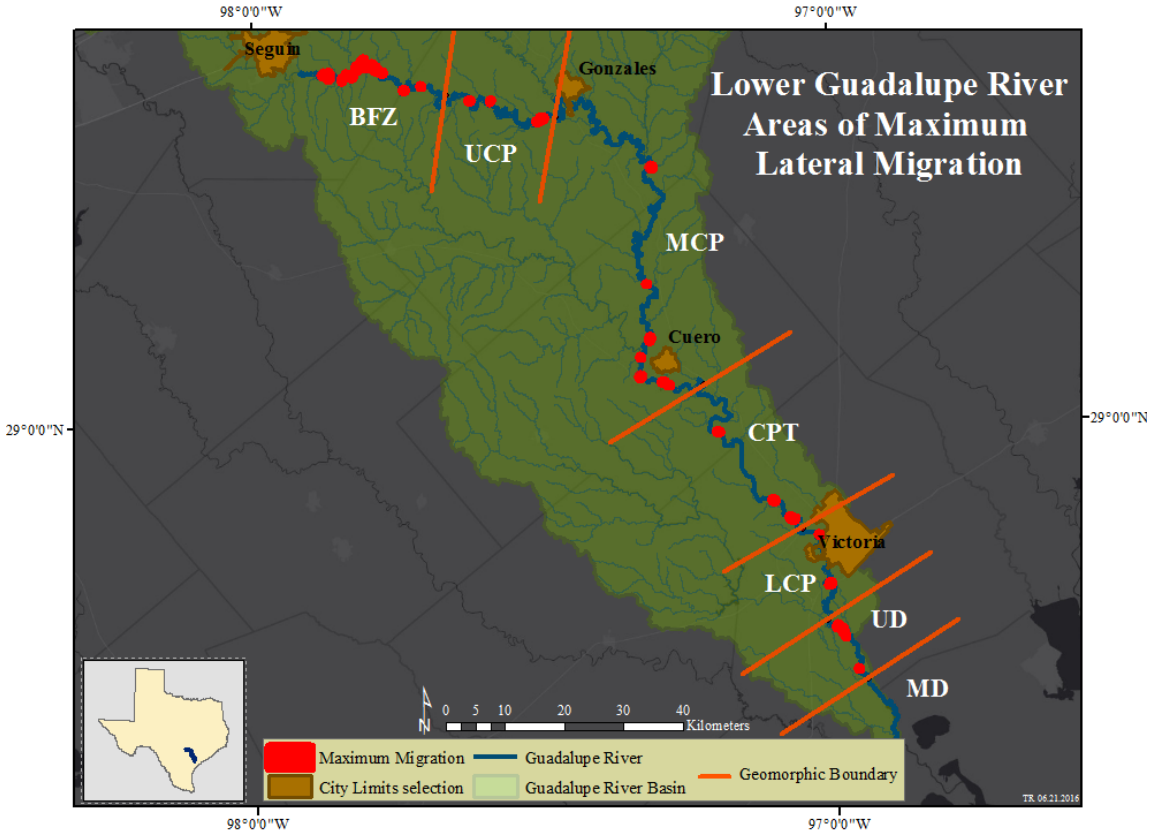


**Figure 25. Map showing areas of maximum lateral migration, in red, for the study period.**

Each sub-reach has several areas of maximum rates of migration, except for the lowest reach. As previous figures have shown, the BFZ has the highest occurrence of maximum rates of migration. Figures 26 through 32 provide details of the rates of migration for each sub-reach. The river is overlain onto the cropped 10 m DEM to provide a visualization of the river valley and surrounding area.

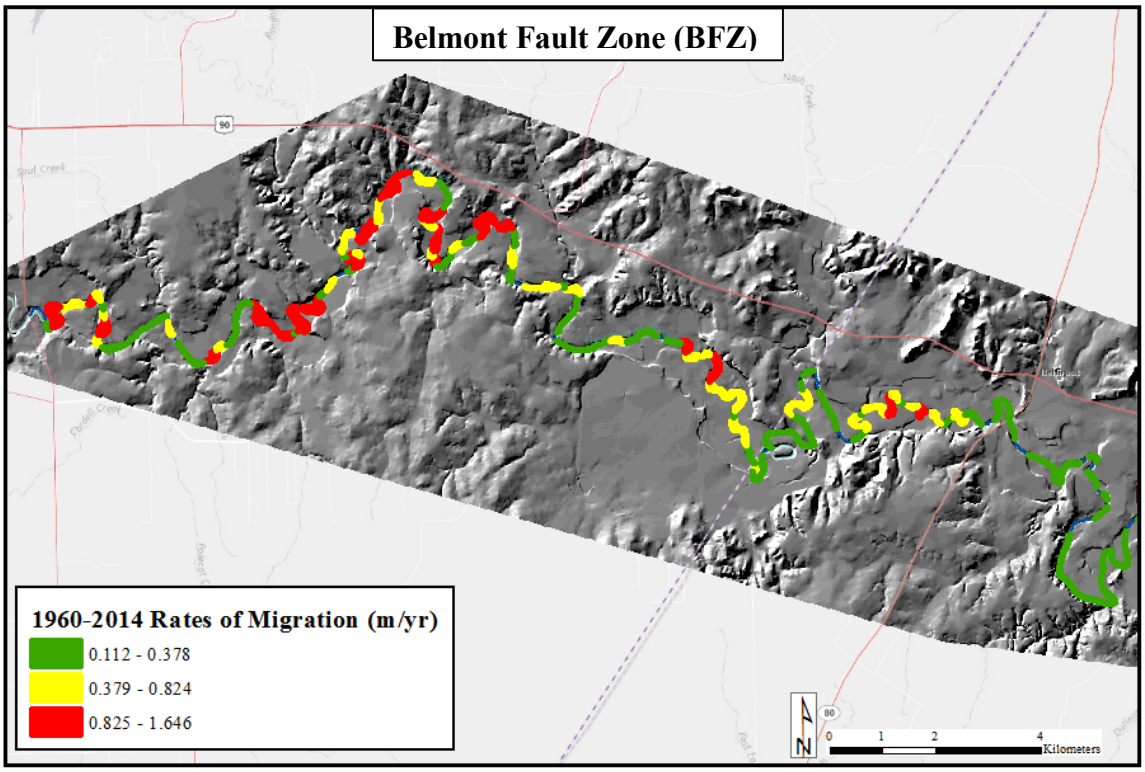


**Figure 26. Rates of migration in the Belmont Fault Zone using a three-class Jenks Natural Break.**

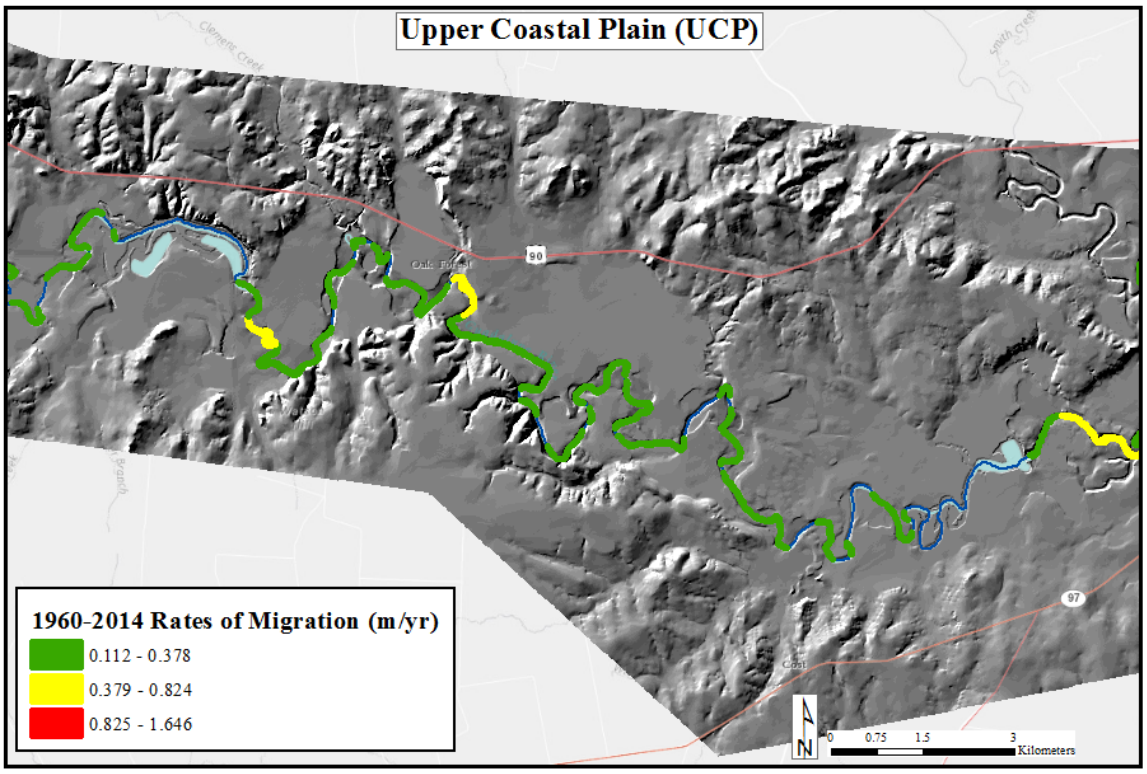


**Figure 27. Rates of migration in the Upper Coastal Plain using a three-class Jenks Natural Break.**

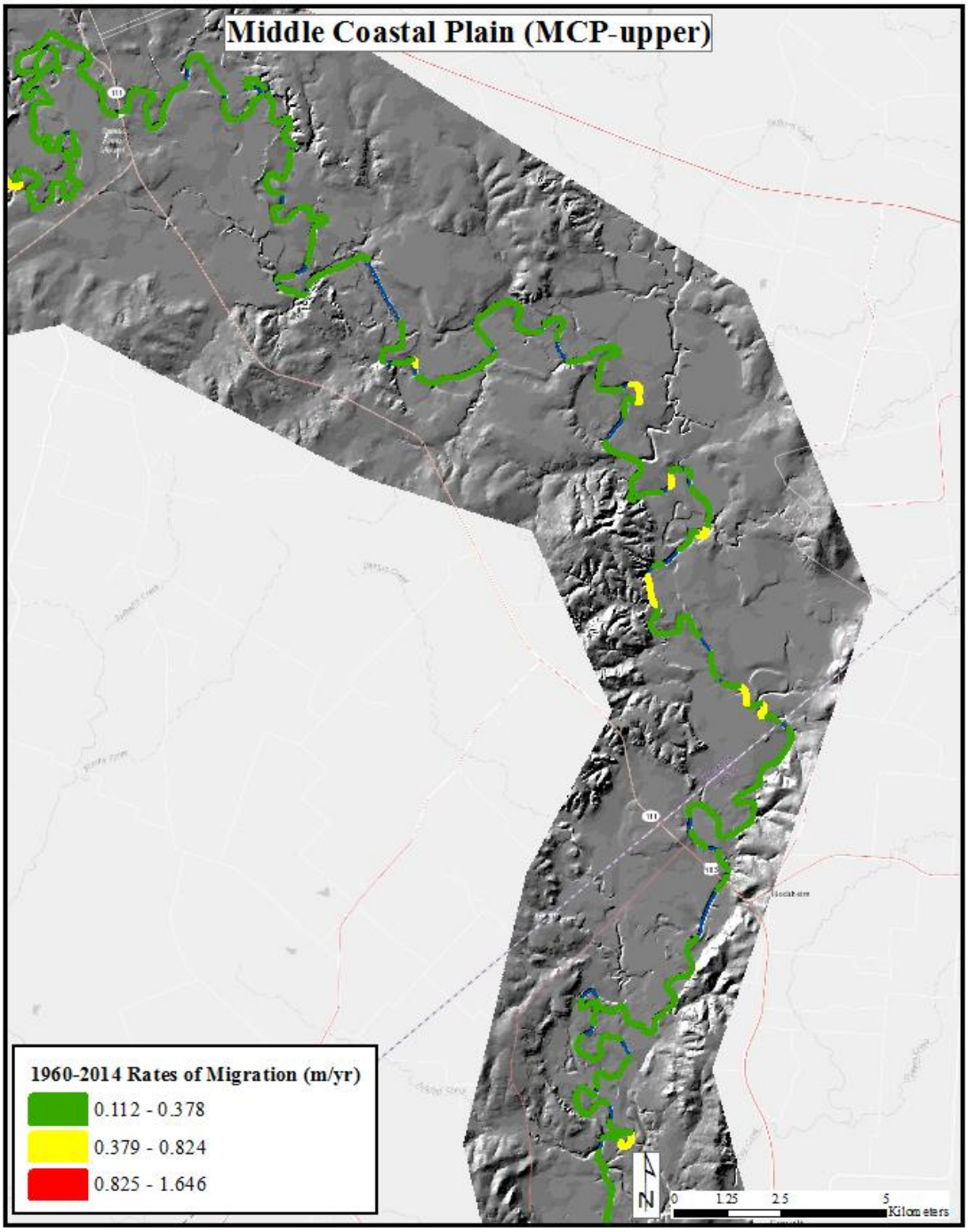


**(a)**

**Figure 28. Rates of migration in the Middle Coastal Plain using a three-class Jenks Natural Break. The zone was divided into upper (a) and lower (b) as a result of the length.**

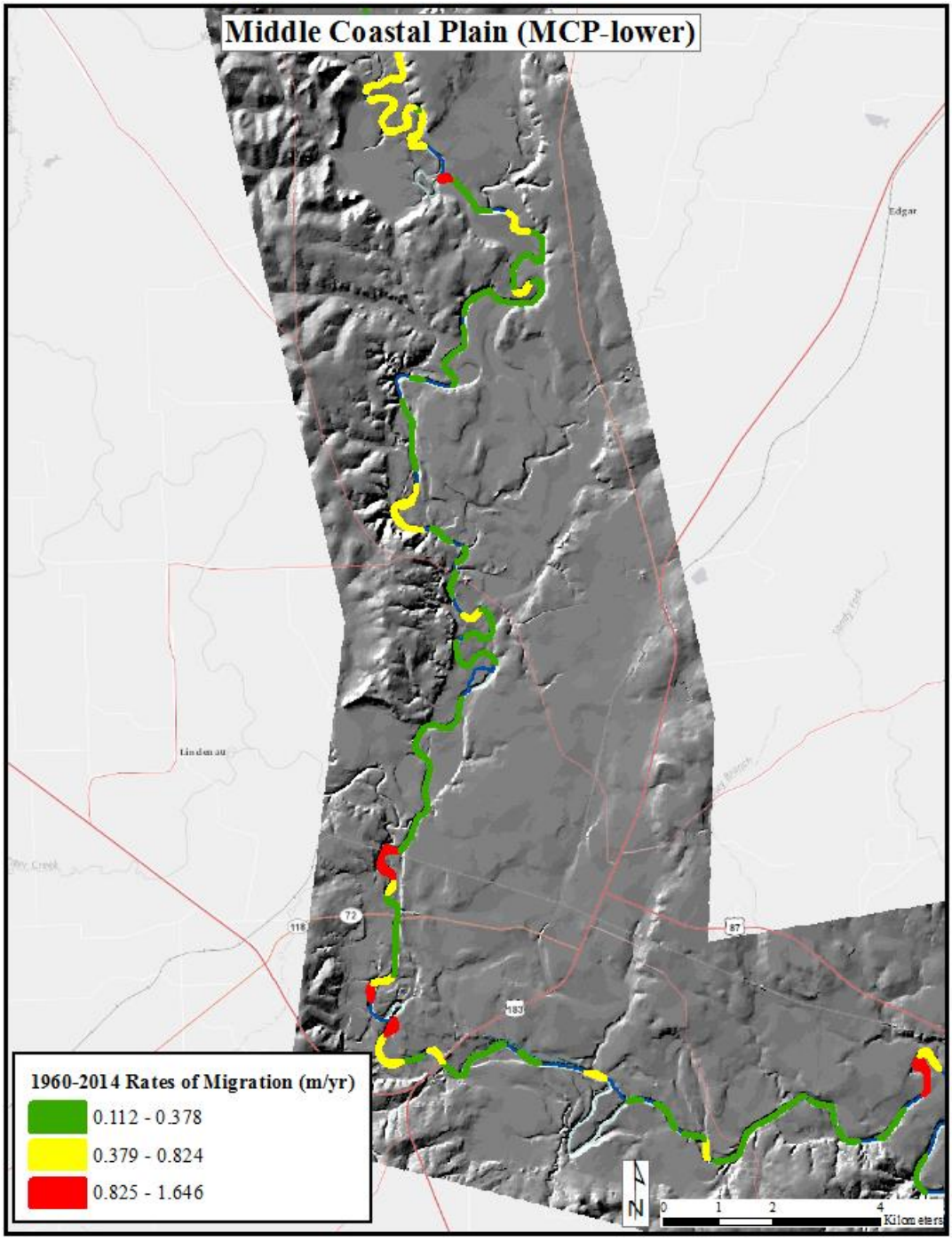


**(b)**

**Figure 28. Continued.**

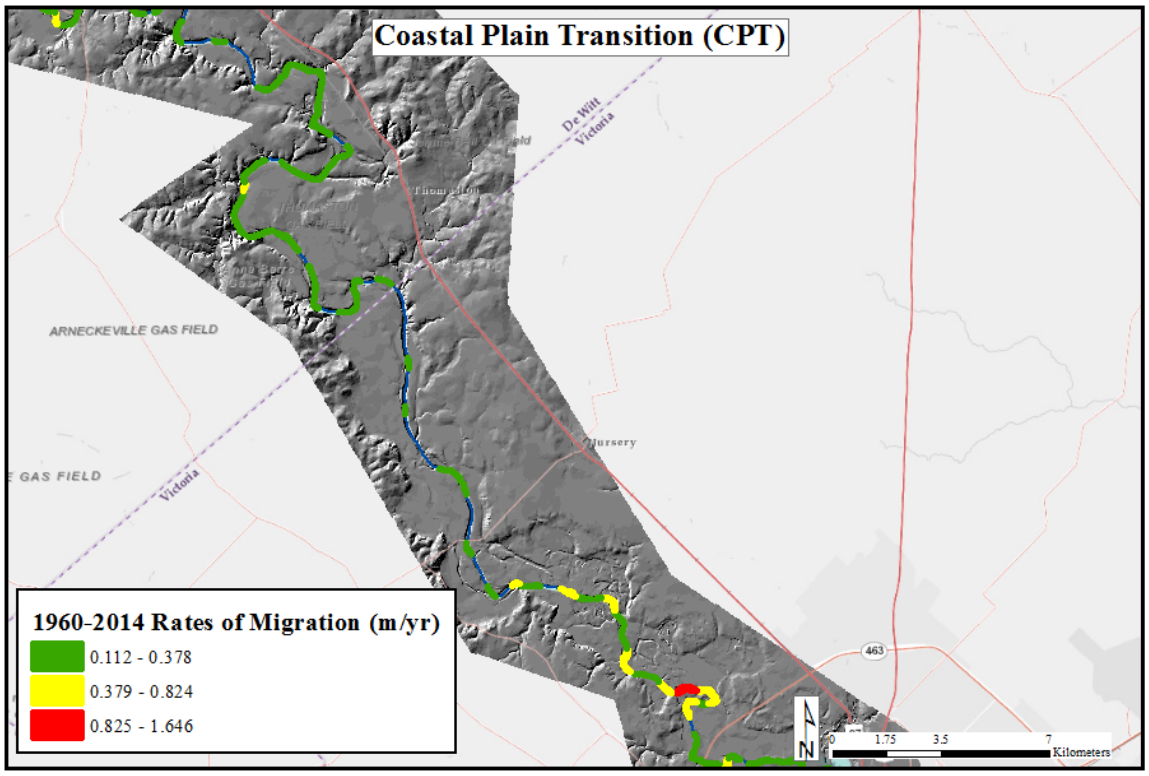


**Figure 29. Rates of migration in the Coastal Plain Transition zone using a three-class Jenks Natural Break.**

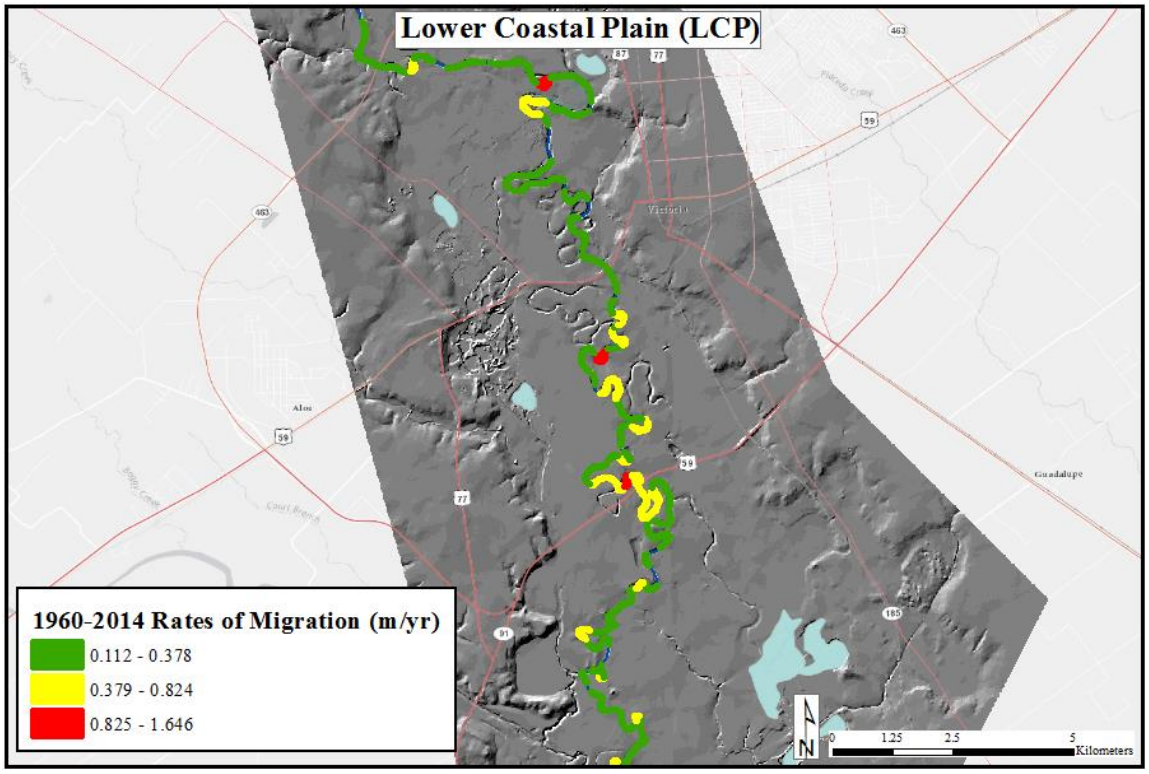


**Figure 30. Rates of migration in the Lower Coastal Plain using a three-class Jenks Natural Break.**

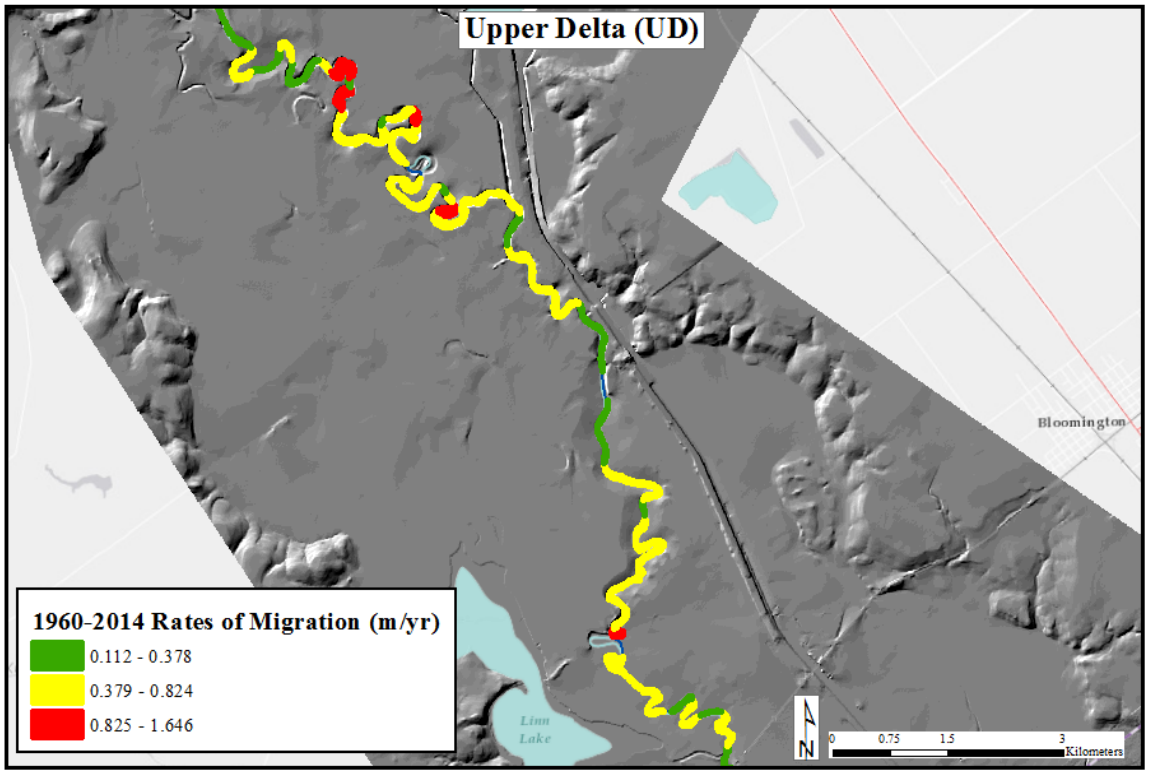


**Figure 31. Rates of migration in the Upper Delta using a three-class Jenks Natural Break.**

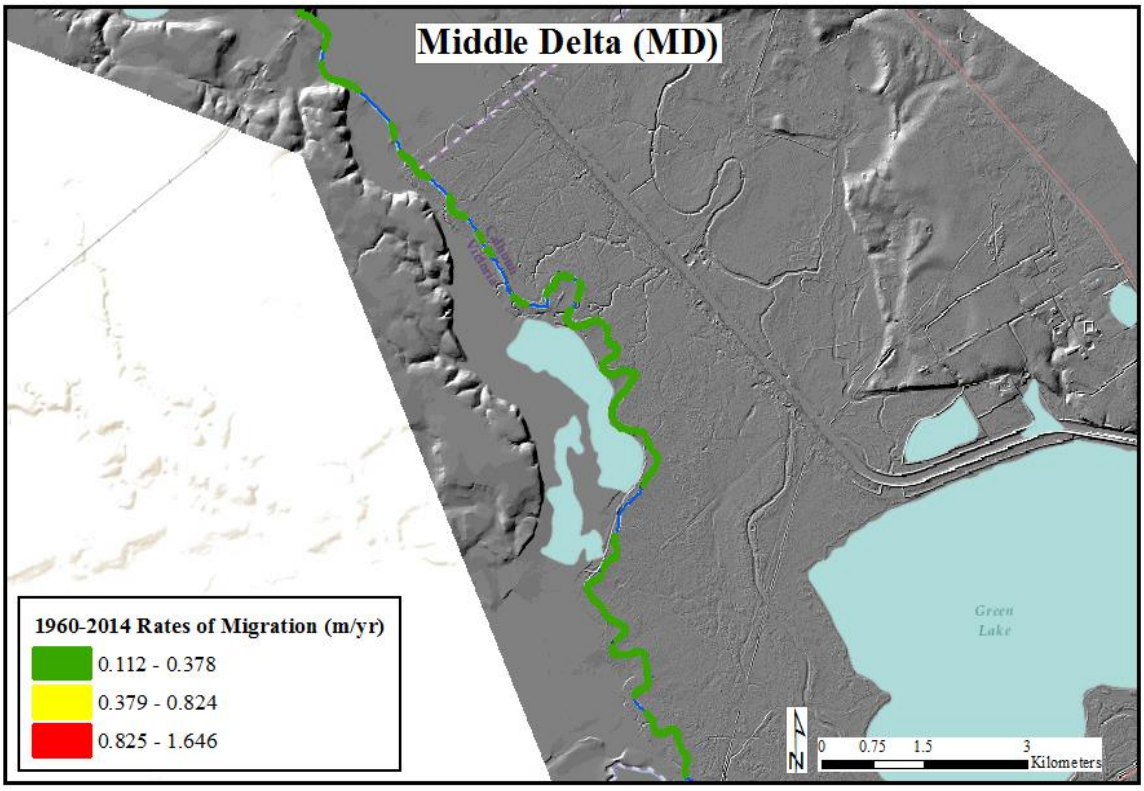


**Figure 32. Rates of migration in the Lower Delta using a three-class Jenks Natural Break.**

Observing areas of migration overlain on a DEM shows the valley confinement present in the BFZ. Confinement and channel constriction influence channel adjustment as seen in the sub-reach. The other sub-reach that stands out is the UD where the valley is wide, but the channel hosts several areas of maximum migration. Other mechanisms drive channel adjustment in this area.

*5.5 ANOVA Statistical Analysis*

To gain a better understanding of possible mechanisms of lateral migration, ten meander bends were designated per reach at random using a GIS for further analysis. The reference for random point generation was the 2014 channel line. The channel line was chosen rather than migration polygons to eliminate bias of analyzing only meanders that have experienced lateral migration. Figure 33 shows the locations of random meander bend points within each sub-reach.

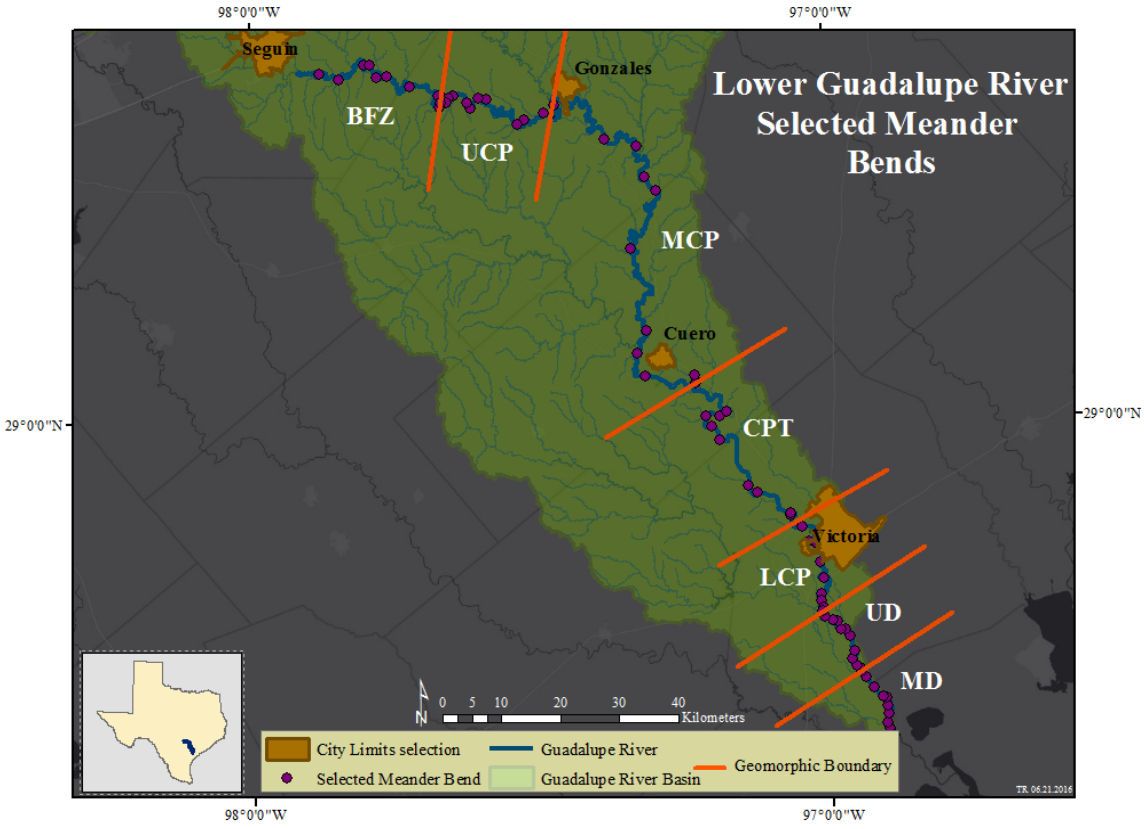


**Figure 33. A map including ten random meander bends per sub-reach used for further analysis.**

Each meander bend was analyzed for various parameters. Table 14 provides an analysis of the relationship between rate of migration and characteristics of the meander bend.

**Table 14. ANOVA comparison of total migration as a function of meander bend characteristics. Rc/W values are averaged for 1960 and 2014.**

| Variable | Rc/W | n | Mean | F-Statistic | P-Value |
|---|---|---|---|---|---|
| Rate of Migration | <2 | 31 | 0.502 | 3.8112 | 0.0271 |
| | 2-3 | 16 | 0.319 | | |
| | >3 | 23 | 0.29 | | |
| | Bend Type | | | | |
| Rate of Migration | Simple | 34 | 0.32 | 3.1998 | 0.0781 |
| | Compound | 36 | 0.46 | | |
| | Outside Bank (OB) Vegetation | | | | |
| Rate of Migration | Yes | 58 | 0.343 | 8.6219 | 0.0045 |
| | No | 12 | 0.621 | | |
| | (OB) Silt-Clay Content (%) | | | | |
| Rate of Migration | 33-50% | 5 | 0.168 | 4.857 | 0.0107 |
| | 51-70% | 11 | 0.62 | | |
| | 71-93% | 45 | 0.364 | | |
| | (OB) Silt Content (%) | | | | |
| Rate of Migration | 15-35% | 25 | 0.304 | 4.7698 | 0.0116 |
| | 35-50% | 13 | 0.614 | | |
| | 50-70% | 32 | 0.367 | | |
| | (OB) Clay Content (%) | | | | |
| Rate of Migration | 15-25% | 11 | 0.532 | 2.4332 | 0.0727 |
| | 25-35% | 37 | 0.366 | | |
| | 35-50% | 13 | 0.246 | | |
| | 50-70% | 9 | 0.527 | | |

### 5.5.1 Vegetation

From the ANOVA, presence of vegetation on the outside bank has the highest p-value, or confidence, in the analysis. It is known that lateral migration often occurs by eroding the outside bank, so characteristics of the outside bend were analyzed. Vegetation was defined as any vegetation taller than a short grass that would be found in a grazing or crop field. When vegetation is present, rates of migration are lower because the associated root system provides stability along an outside bank. Different types of vegetation provide more or less stability depending on size and type of plant and the root system. This analysis did not account for type, only presence.

### 5.5.2 Bank Composition

Outside bank composition, measured by percentage of silt-clay in the soil, has the second most significant relationship. Content percentages were grouped into three classes where it was found that silt-clay composition of 51-70% has the highest rates of migration. Clays are cohesive and can resist high shear stresses because of the geotechnical properties it possesses. Silts are cohesive as well, but to a lesser degree than clay. The remaining percentage bank composition is classified as sand, which is non-cohesive. Because it is assumed that sand plays a minimal role in bank stability for the chosen meanders, only silt and clay were analyzed.

To determine if silt or clay has more influence, the two were analyzed separately. A 35-50% silt composition has higher rates of migration whereas 15-25% and 50-75% clay composition relates to higher rates of migration. Separately analyzing the two

confirms that the presence of both strengthens a bank. None of the banks had a homogenous silt or clay content, so the relationship of silt or clay alone to lateral rates of migration is unknown for this study.

### 5.5.3 Type of Bend and Radius of Curvature

Results from the ANOVA show that radius and curvature and type of bend have significant relationships with lateral rates of migration. Simple and compound types of bends have significantly different mean rates of migration. Compound bends have higher rates, which can be related to dynamic shear stresses because flows do not follow a typical sinuous curve. Compound versus simple bends are related to the size and tightness of the bend, so type of bend and Rc/W measurements were compared, shown in Table 15.

**Table 15. ANOVA of average Rc/W values versus type of bend. Rc/W values are averaged for 1960 and 2014.**

| | Type of Bend | n | Mean | F-Statistic | P-Value |
|---|---|---|---|---|---|
| Average Rc/W | Simple | 34 | 2.31 | 0.2870 | 0.5939 |
| | Compound | 36 | 2.45 | | |

Results show no significant difference in the means of Rc/W when grouped by simple versus compound bends. The average Rc/W value is 2.38, which is in the generally accepted range for maximum migration. Maximum migration, however, occurs between one and two for the lower Guadalupe River.

Rc/W is grouped according to the findings of Hickin and Nanson (1984) where a ratio of 2-3 has the highest rates of migration. The results show that a ratio less than two has higher rates of migration. Figure 34 compares the relationship between Rc/W and rate of migration data from Nanson and Hickin (1986) to the lower Guadalupe River data.

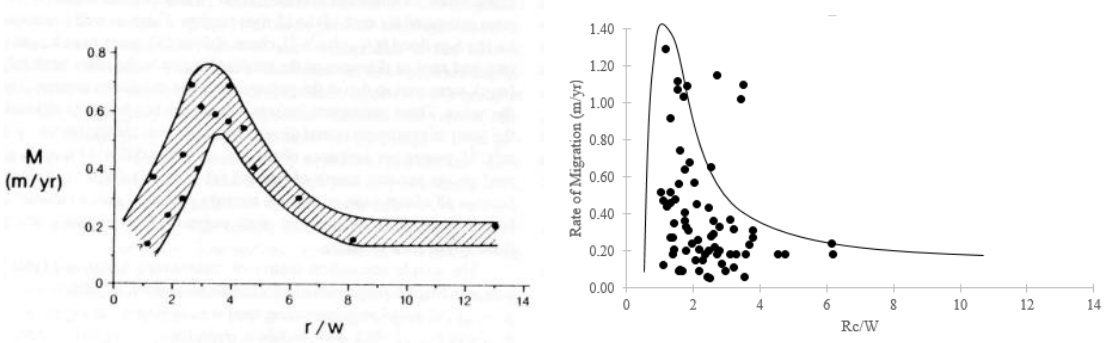


**Figure 34. Ratio of radius of curvature and width to rate of migration for the Beatton River, Canada from Nanson and Hickin (1983) (left) to the lower Guadalupe River (right).**

Although the maximum rates of migration occur at values less than two for the lower Guadalupe River, the scatterplot has a similar shape to the Beatton River, Canada.

My data have several values for lower rates of migration, where Nanson and Hickin do not. This can be attributed to different sample sizes as well as different river systems.

*5.6 ANOVA for Sub-Reaches*

An ANOVA was also run to determine differences in geomorphic variable per sub-reach. The ANOVA confirms what figures above determined; a significant difference in rates of migration exists between sub-reaches. Table 16 presents the results of the analysis.

**Table 16. ANOVA comparison of bend morphology as a function of Geomorphic Zone. Average values for 1960 and 2014 for 70 random meander bends.**

| Variable | Reach | n | Mean | F-Statistic | P-Value |
|---|---|---|---|---|---|
| Rate of Migration | BFZ | 10 | 0.596 | 4.4151 | 0.0009 |
| | UCP | 10 | 0.221 | | |
| | MCP | 10 | 0.391 | | |
| | CPT | 10 | 0.324 | | |
| | LCP | 10 | 0.382 | | |
| | UD | 10 | 0.661 | | |
| | MD | 10 | 0.16 | | |
| Average Rc/W | BFZ | 10 | 2.42 | 2.285 | 0.0465 |
| | UCP | 10 | 2.04 | | |
| | MCP | 10 | 2.36 | | |
| | CPT | 10 | 2.62 | | |
| | LCP | 10 | 2.6 | | |
| | UD | 10 | 1.54 | | |
| | MD | 10 | 3.09 | | |

**Table 16. Continued.**

| Variable | Reach | n | Mean | F-Statistic | P-Value |
|---|---|---|---|---|---|
| Sinuosity | BFZ | 10 | 1.507 | 0.8624 | 0.528 |
| | UCP | 10 | 1.508 | | |
| | MCP | 10 | 1.369 | | |
| | CPT | 10 | 1.199 | | |
| | LCP | 10 | 1.339 | | |
| | UD | 10 | 1.368 | | |
| | MD | 10 | 1.234 | | |
| Slope | BFZ | 10 | 0.097 | 0.942 | 0.4714 |
| | UCP | 10 | 0.98 | | |
| | MCP | 10 | 0.057 | | |
| | CPT | 10 | 0.153 | | |
| | LCP | 10 | 0.482 | | |
| | UD | 10 | 0.021 | | |
| | MD | 10 | 0.017 | | |
| Average channel width | BFZ | 10 | 36.02 | 5.098 | 0.0003 |
| | UCP | 10 | 45.15 | | |
| | MCP | 10 | 45.19 | | |
| | CPT | 10 | 53.68 | | |
| | LCP | 10 | 41.83 | | |
| | UD | 10 | 41.9 | | |
| | MD | 10 | 36.89 | | |

Average Rc/W and average channel width are significantly different between sub-reaches, whereas sinuosity and slope are not. Because significant differences occur in rates of migration between sub-reaches, it can be determined that sinuosity and slope, alone, are not mechanisms related to rates of migration, whereas Rc/W and average channel width are.

# 6. DISCUSSION

## *6.1 Lateral Rates of Migration*

### 6.1.1 2010-2014 Rates of Migration

Discharge and rates of migration throughout the study period were shown to have a relationship, trending in a similar pattern. The study period 2010-2014, however, had a very low average discharge and the highest rates of migration for the study periods. A major drought occurred across Texas during 2011 and 2012. As water becomes scare from lack of precipitation and enhanced evapotranspiration, the result is lower flows in rivers across the affected area. Lower flows result in lower river stages, and a lower stage means that banks that are normally wet or submerged are now dry.

Water, at the right velocities, will help stabilize a river bank as a result of increased pore water pressure in the bank soils. A drought means that areas that had increased pore water pressures rely solely on cohesion. Although cohesive, slip faces increase as fractures occur from a lack of water to bind the cohesive materials. Increased fractures results in bank instability. When unstable, failure of river banks can occur in the form of slumping as seen in Figure 35.

**(a)**

**(b)**

**Figure 35. (a, b) Slumping along an outside bank on the Guadalupe River near Cuero, TX. (December 5, 2015).**

Undercutting of banks is another type of bank failure can occur as a result of drought and lower river levels. A cut- bank typically has high angle slopes exposed, and a toe slump underwater that is a result of previous erosion. As river levels drop, the river will start to erode the toe slump, destabilizing the upper cut-bank that eventually initiates collapses. Collapsing banks can produce exaggerated rates of migration because the process is immediate rather than eroding away at a bank over the course of several years. Figure 36 provides an example of undercut banks near Cuero, TX.

**Figure 36. Example of collapsing banks as a result of undercutting. Photo near Cuero, TX. (December 5, 2015).**

### 6.1.2 Upper Delta and Middle Delta

To identify other mechanisms controlling lateral migration, I looked at adjacent sub-reaches; the UD and MD. The UD has the second highest rates of migration, and the MD has the lowest. This is the result of the proximity to the Gulf of Mexico; a base-level. Low rates of migration, seen in the MD, are explained by tidal fluctuation influences the river. Tides limit downstream flow, and can cause flow reversal that results in standing water. Standing water lacks energy to promote lateral migration, thus, aggradation dominates and rates of migration are significantly lower in this area. The rise of sea level also causes aggradation into the delta, inhibiting the river to incise (Donaldson et al., 1970 ; Blum and Aslan, 2006 ).

The relationship between the river and the ocean is not the only explanation of migration in these reaches. The reason for the contrast in rates of migration between the two adjacent reaches is a result of a zone of subsidence. Ouchi (1985) investigates the influence of the Post-Vicksburg flexure zone located near the confluence of Coleto Creek, 32 km above the mouth of the river in the UD reach. The flexure is clearly seen in Figure 37 as a small concave zone near the end of the reach.

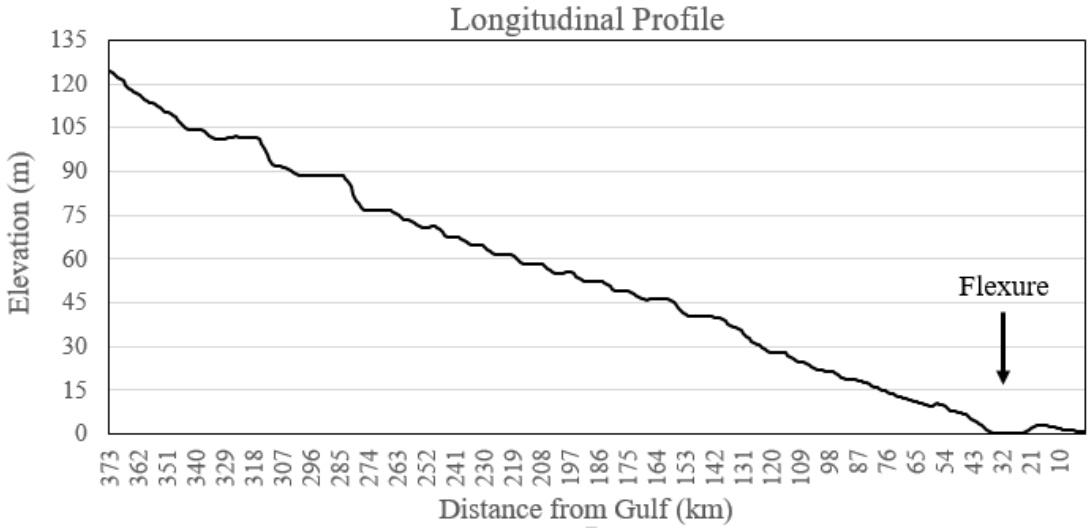


**Figure 37. Longitudinal profile showing Post-Vicksburg flexure zone near the end of the reach.**

Above the flexure, higher valley slope increases sinuosity in the reach of the river because it is adjusting to toward equilibrium. Adjustment results in higher rates of migration, which the UD demonstrates. Just below the flexure in the MD, the slope is nearly flat, and the stream tends toward a straight path where aggradation dominates and limits the rates of migration. Base level in the MD is the Gulf of Mexico, so the river does not adjust much here because elevation is close to sea-level through the reach.

### 6.1.3 Belmont Fault Zone and Upper Coastal Plain

At the top of the study reach, channel adjustment occurs in the BFZ and UCP; adjacent reaches. The BFZ has the highest rates of migration and the UCP has the second lowest rates of migration. The BFZ has a very confined valley compared to other

sub-reaches, which contributes to high rates of migration. Confined valleys can restrict meander formation and movement as the channel nears a valley wall.

The geology is another factor that can restrict movement. In the BFZ, alluvial terraces dominate the valley walls. Walls are erodible, but less so than the alluvium in which the channel resides. In the lower BFZ, the valley constricts the channel and results in increased rates of migration upstream. A point of constriction will result in a straighter segment of river through the constriction, and widening above and below. This constriction is associated with Eocene aged sediments that are less erodible than the alluvial terraces and fill of the Quaternary.

Another possible influence on high rates of migration is the construction of the FM 1117 bridge. The bridge was constructed in 1984. Some of the highest amounts of migration are directly downstream of the bridge. It is unclear if it is the direct result of the bridge, or other factors within the zone.

Geographic location of the BFZ is another factor affecting the sub-reach. The BFZ is situated below the Balcones Escarpment by ~22 km. The river comes off of the steep-sloped escarpment onto the flat coastal plain where is has energy that must be dissipated. Dissipation comes in the form of aggradation and erosion. The processes can explain some of the migration the area is experiencing, however a stark change occurs upon entering the adjacent sub-reach. Although the escarpment is a factor, the active fault zone within the sub-reach has more impact on the zone. Any movement produced by the fault can affect the channel up and downstream, although upstream is

more active. Downstream effects of the fault may be dampened as a result of the proximity to the dam.

Following the concept of dynamic equilibrium, the high rates of migration in the BFZ can also be attributed to dams up and downstream of the zone. The construction of a dam will change the base level that the segment of river is trying to achieve. A change in base level will cause aggradation upstream of the impoundment and erosion downstream. Adjustment can occur for decades after construction, however, rapid change typically occurs shortly after construction because the channel must immediately adjust to a new flow regime and sediment load. Six dams, four upstream of the BFZ and two within the UCP affect the sub-reaches. The dams were all built between 1928 and 1931, so adjustment should be less significant than after the initial construction. This can explain the low rates of migration in the UCP, where it appears the two dams are in equilibrium with each other and the river channel.

*6.2 Dams*

It is unknown how much adjustment occurred within the river channel directly after completion of the two dams, Lake Gonzales and Wood Lake, in the UCP sub-reach. This study, however, starts analysis in 1960, thirty years after completion, and sees very little adjustment downstream of the dams. Figures 38 and 39 provide the rates of migration for 1960-2014 below both dams. I can only quantify lateral adjustment and do not account for any vertical adjustments of the river channel.

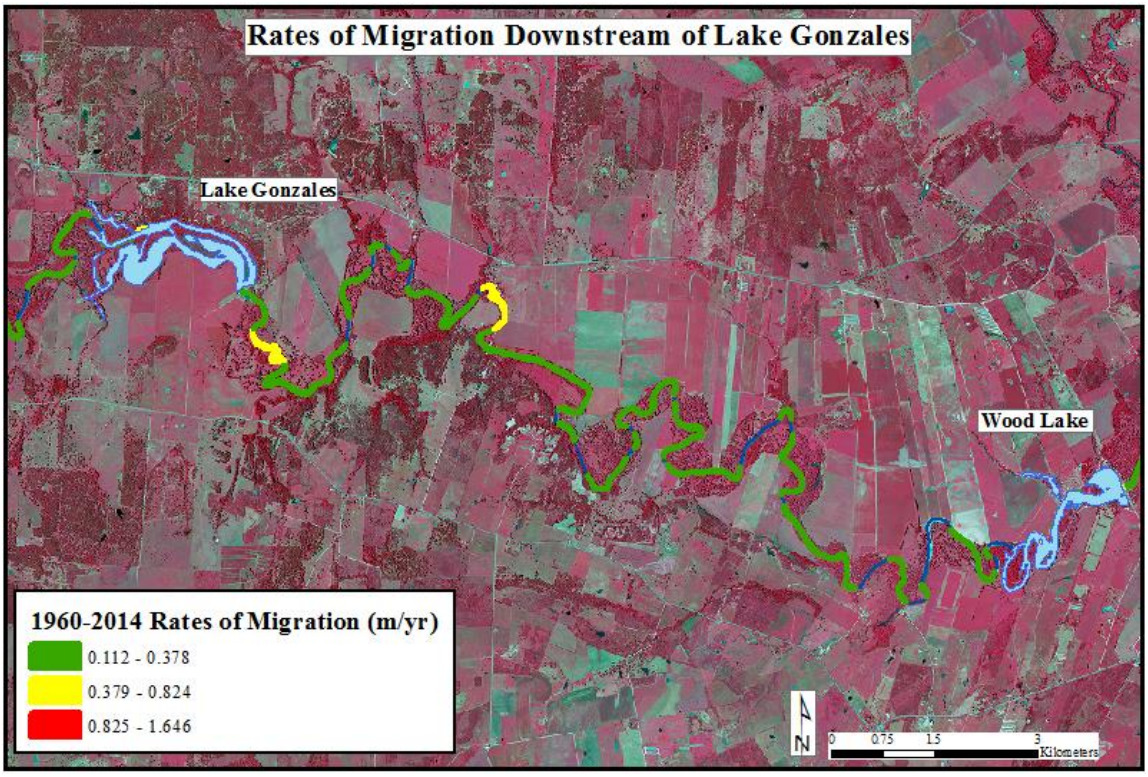


**Figure 38. Rates of migration downstream of Lake Gonzales.**

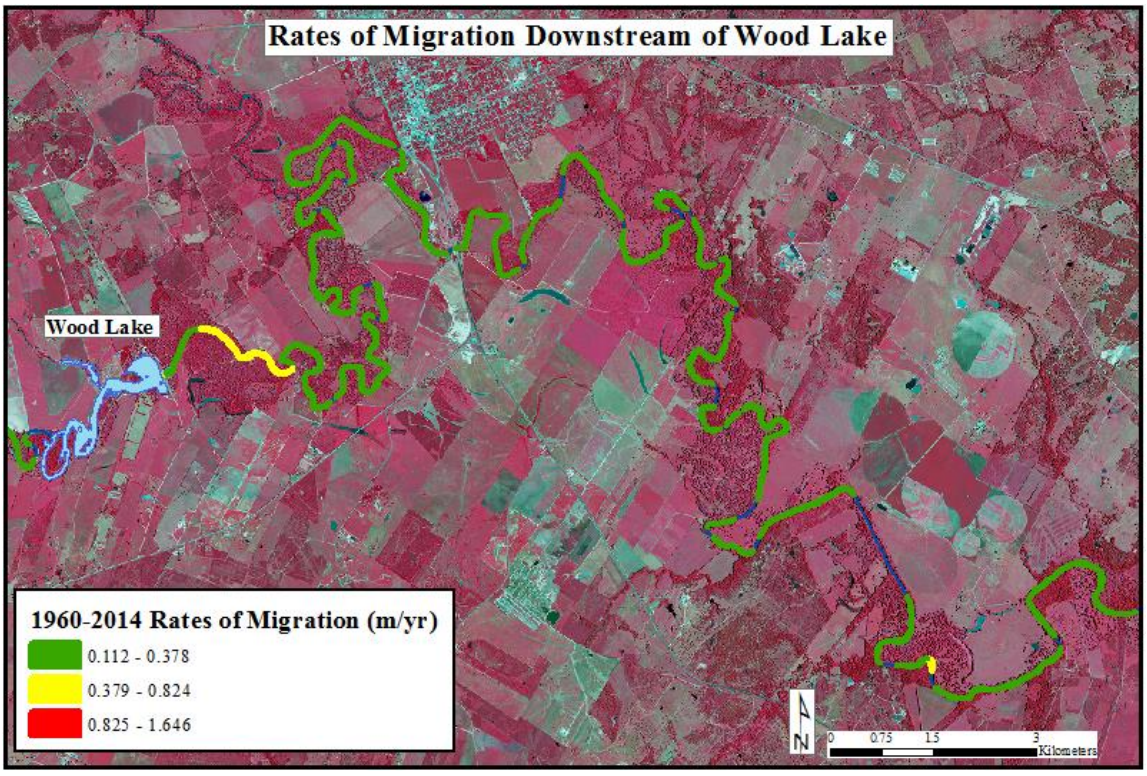


**Figure 39. Rates of migration downstream of Wood Lake.**

Minor lateral adjustment is seen downstream of the dams. Philips (2007) states that it takes about 55 km for the river to regain the desired sediment load to minimize channel adjustment downstream of a dam. The two dams within the study reach are about 30 km apart. The proximity to Wood Lake from Lake Gonzales can explain minimal changes downstream because the local base level is relatively close. The relative stability below Wood Lake, however, is not explained by a local base-level.

The stability below Wood Lake can be contributed to the altered flow regimes controlled by dam releases. Dam releases dampen peak flows and increase base-flows creating a more moderate flow regime for the river. Although peak flows are dampened,

hydropeaking occurs as dams release water for hydropower generation. Hydropeaking creates daily pulses of increased flows that cause daily stage height changes. The effects of hydropeaking, however, depend on the volume of water being released. Wood Lake is relatively small, so daily fluctuations are minimal and a moderate flow regime dominates which enhances channel stability.

The size of the dam needs to be considered when observing the effects of a dam on a river system. Lake Gonzales and Wood Lake are very small compared to the dam at Canyon Lake, ~150 km upstream. Canyon Lake has a storage capacity of 728,400 acre feet compared to the capacity of Lake Gonzales at ~7,500 acre-feet and Wood Lake at ~4,000 acre-ft. Phillips (2011) states that about 20% of the flow that reaches the Gulf of Mexico is attributed to Canyon Lake releases. The author also states that it is difficult to attribute channel change to the dam because of the numerous geomorphic factors affecting the river before taking the influence of the dam into consideration. Although it is difficult to quantify effects from dams within the study reach, the artificial moderate flow regimes contribute to channel stability on the lower Guadalupe River.

### *6.3 Meander Cut-Offs*

Although meander cut-offs were not used for analysis of the rate of migration, the process is important when considering the stability of a river system. Stølum (1996) suggests that meandering river systems develop through opposing processes where lateral migration increases sinuosity and meander cut-offs decrease it. The author suggests that meander cut-offs create short periods of dampened rates of migration

because the river straightens to the path it wants to take. The effect of a cut-off to the river system is dependent, however, on the state of the system itself. In a chaotic, instable state, cut-offs bring the system toward a more stable state, whereas cut-offs that occur in a stable state tend toward instability. The author relates high sinuosities to an active system, so a system such as the lower Guadalupe should be active and, therefore, unstable.

Hooke (2007) suggests that high sinuosity, however, does not necessarily relate to activity and stability. The lower Guadalupe River is an example of this. The channel in tortuous in nature, but has had only six meander cut-offs in the last 54 years. Although geologically that is a short time period, the process of meander cut-offs does not follow what others have seen. Stølum (1996) suggests an avalanching effect once a cut-off has occurred. Bends around the initial cut-off will change drastically in a short time period. This does not seem to hold true for the lower Guadalupe River.

The river is scarred with oxbows and meander scrolls which indicate a historically active channel. Dating the oxbows and meander scrolls would give insight into the temporal activity of the channel, however, that was outside the scope of this project. Currently the channel is focused on lateral migration. Some areas of the study reach are very active, but the areas are increasing the size of the meander bend rather than termination of growth through a cutoff.

Throughout the study reach, only six meander cut-offs and one avulsion have occurred. Four occurred during the highly active flood period, 1995-2004. Cut-offs may have been the direct result of a high discharge. Chute cut-offs, the more immediate

type, are typically the result of high discharges. Only one chute cut-off appears to have occurred during the active flood period of 1995-2004. The type of cut-off, however, is assumed by observing aerial imagery, thus, a visually identified neck cut-off could have been accelerated as a result of chute development during or post-flood.

The avulsion that occurred during the same 1995-2004 period was initially a result of the decommission of hydropower plant in 1965 (Godfrey and Dowell, 1968). Turbines no longer let the river pass through the structure, so it inhibited flow, creating a backwater. The structure created an area of high pressure above the dam, initiating groundwater flow paths as water moved from high pressure to the lower pressure, below and around the structure. A combination of flow path development, soil saturation, and high-flow events contributed to the channel avulsion around the flow structure. The channel now completely avoids the structure.

The two cut-offs and the avulsion occurred within the same sub-reach, the MCP. The cut-offs occurred after the dam was decommissioned and the channel started to adjust. Proximity of the cut-offs to each other may have been a result of the channel adjusting to each major change. The fourth cut-off during the same time period occurred in the lower part of the UD reach. The upper part of the UD reach experienced another cut-off in the following study period, 2004-2010. In this sub-reach, both were neck cut-offs. A neck cut-off is more indicative of meander growth and termination. Because the UD is highly active, cut-offs of lateral meanders are expected as the sub-reach continues to adjust.

Another neck cut-off occurred in the lower part of the BFZ reach during the 2004-2010 study period. In the same study period, a neck cut-off occurred in the lower part of the BFZ reach. The cut-off occurred just below the areas of maximum migration. Because the zone is very active, the cut-off may be a result of channel adjustment. A flood also occurred in 2013 that could have contributed to the cut-off. The BFZ has the highest sinuosity by sub-reach at 3.07. Stølum's (1996) model finds that a bend will tend toward a steady-state value of 3.14. The author looks at an individual bend, however, rather than several in succession.

Sinuosity, along with other planform variables, is difficult to account for in a single bend because each bend is affected by adjacent meanders. It is thus important to use sinuosity as an indicator and view the river and each bend as a system. One must also understand the importance of the indicator and recognize the relation to and role within the system.

*6.4 Radius of Curvature*

Indicators of river stability and the consideration of factors affecting different sites are important. Nicoll and Hickin (2010) look at the difference in Rc/W measurements for confined and freely migrating meanders. Confined valleys dominate the Canadian prairie where the authors have study sites. Confined meanders have higher Rc/W ratios whereas freely meandering have lower, closer to the accepted ratio between two and three.

The lower Guadalupe River is a freely meandering system in the sense that the valley is wide enough so as not to confine the river. The river is under-fit for the valley which allows it to meander and migrate freely apart from dams and other channel obstructions. Although the river has free-meanders, Rc/W ratios are lower than what the authors found for Canadian Prairie rivers. Because the river is under-fit, having a larger valley than the current size of river needs, large meanders can develop which in turn develops compound bends. Compound bends form because flow velocities decline and reverse if the distance is too large through a meander bend, resulting in the formation of another bend within the larger bend.

Numerous compound bends characterize the lower Guadalupe, resulting in a tortuous river with sinuosities above 2 for all sub-reaches. Sinuosities in Nicoll and Hickin's study area are closer to regular; between 1.1 and 1.8. The difference in average sinuosity influences Rc/W measurements and could account for the difference between the Canadian Prairie study site and the lower Guadalupe River.

Results for the lower Guadalupe River are also compared to results to a tortuous river system in Puerto Rico where highest rates of migration occur at an average Rc/W of 2.42 (Alvarez, 2005). Results of two different studies on the Brazos River, another Texas Coastal Plain river, present similar results. Gillespie and Giardino (1997) found rates of migration were highest for bends with a Rc/W ratio of 2.5-3.5. Lee and Giardino (2011) found similar results where ratios of 2-3 experienced the highest rates of migration.

Rates of migration were greatest with an Rc/W measurement of <2 on the lower Guadalupe River. This can be attributed to an overall stable channel throughout the reach. Average rate of migration for a Rc/W value <2 is 0.5 m/yr compared to 0.32 m/yr at a ratio of 2-3. Major changes can occur in one bend over 54 years, and that can bias the Rc/W ratio. Each bend is dependent on local factors, outside of channel planform. Vegetation and soil composition can control the migration of a meander bend more than the geometry of the channel itself. The ratio should be used as an indicator of the stability of the river, but each bend should also be observed independently. To better understand the relationship that the Rc/W ratio has on the lower Guadalupe River, each meander bend should be quantified. The ratios of a larger compound bend and single simple bends within the compound bend should also be analyzed to understand the compounding effect.

# 7. CONCLUSION

The purpose of this study is to understand and analyze the migration of meanders as a response to systematic changes along the lower Guadalupe River. To achieve this, rates of migration were calculated along the lower Guadalupe River over several temporal intervals. Rates were determined for the entire reach as well as for predetermined sub-reaches. Mechanisms of channel adjustment were also investigated to determine what the major controls of lateral migration are on the lower Guadalupe River.

Overall the channel is stable in the sense that it appears it can adjust well to dynamic discharges. A 54-year time period is limited, but it provides a perspective on the stability of the channel. Stable refers to dynamic stability, so while one section of channel may be very active, the reach as a whole adjusts to keep the system relatively stable within itself. When looking at the 380 km reach, the river experiences minimal rates of migration at an average of 0.36 m/yr over the 54-year period. Unstable areas are noticeable when observing the river at the sub-reach scale. The BFZ and UD are the most unstable sub-reaches with average rates of migration at 0.53 and 0.47 m/yr respectively. The most stable reaches are the UCP and MD with average rates of migration at 0.22 and 0.2 m/yr respectively.

Mechanisms contributing to the rates of lateral migration are the presence of vegetation on the outside banks and a high silt-clay content of the bank. Other mechanisms are the influence of dams, especially in the BFZ and UCP sub-reaches. However, the influence of Canyon Lake, ~150 km outside the study reach, is observed

throughout the 380 km reach. Moderate flows produced by releases at the dam contribute to the channel stability of this reach of river. A lack of channel change is missing directly downstream of the two dams within the UCP reach. This is a result of the artificial moderate flow regimes, as well as the installation of the dam 85 years ago that has allowed time for the channel to equilibrate.

The zone of subsidence in the UD and MD is another mechanism affecting channel change. The flexure zone is active, so channel adjustment occurs in response to any changes. The effect of rising sea-level, also an active process, contributes to channel change in the lower sub-reaches because relative base-level is changing.

Several factors are unaccounted for in this study that may contribute to rates of lateral migration. First, I made assumptions that bank composition is homogeneous through a soil column. To better understand the relationship between soils and a meander bend, field sampling of soil type, pore-pressure, silt-clay content, and soil stratigraphy should be quantified in several locations along a meander bend to form a realistic understanding of the bend.

Another factor to account for is the channel hydraulics through a meander bend. It is generally understood how water will flow through various shaped bends, however, that assumes the channel bottom follows a standard geometry. Sediment movement, type and size vary throughout a meander bend and will affect the hydraulics within the bend. Documenting the bathymetry of a meander bend and several successive bends can lead to important geomorphic factors that have not been considered to effect lateral migration.

My study provides a broad overview on the stability of the lower Guadalupe River using rates of lateral migration. I use three different scales to gain insight into the relationship between a single meander bend, the sub-reach it is in, and the entire 380 km reach. Each reach affects one another, so it is important to consider the mechanisms working at different scales. A future study can include the mechanisms I did not account for and include a field work component that will enhance and advance the work of this study.

# REFERENCES


Ahnert, Frank. "Equilibrium, Scale and Inheritance in Geomorphology." *Geomorphology* 11, no. 2 (1994): 125-140.

Alvarez, Aldo. "Channel Planform Dynamics of an Alluvial Tropical River." Dissertation, Texas A&M University, (2005): 1-98.

Association, Texas State Historical. "Texas Almanac: Rivers." (2010).

Bagnold, Ralph Alger. *Some Aspects of the Shape of River Meanders*. USGS, (1960): 135-144.

Baker, Victor R. "Flood Hazards Along the Balcones Escarpment Incentral Texas Alternative Approaches to Their Recognition, Mapping, and Management." *Bureau ofEconomic Geology Circular* 75, no. 5 (1975): 1-20.

Baker, Victor R. "Hydrogeomorphic Methods for the Regional Evaluation of Flood Hazards." *Environmental Geology* 1, no. 5 (1976): 261-281.

Baker, Victor R. "Stream-Channel Response to Floods, with Examples from Central Texas." *Geological Society of America Bulletin* 88, no. 8 (1977): 1057-1071.

Baz, Ibrahim, Abdurrahman Geymen and Semih Nogay Er. "Development and Application of Gis-Based Analysis/Synthesis Modeling Techniques for Urban Planning of Istanbul Metropolitan Area." *Advances in Engineering Software* 40, no. 2 (2009): 128-140.

Bizzi, Simone and David N Lerner. "The Use of Stream Power as an Indicator of Channel Sensitivity to Erosion and Deposition Processes." *River Research and Applications* 31, no. 1 (2015): 16-27.

Blum, Michael D and Andres Aslan. "Signatures of Climate Vs. Sea-Level Change within Incised Valley-Fill Successions: Quaternary Examples from the Texas Gulf Coast." *Sedimentary Geology* 190, no. 1 (2006): 177-211.

Bracken, Louise J and John Wainwright. "Geomorphological Equilibrium: Myth and Metaphor?" *Transactions of the Institute of British Geographers* 31, no. 2 (2006): 167-178.

Brewer, Cynthia A and Linda Pickle. "Evaluation of Methods for Classifying Epidemiological Data on Choropleth Maps in Series." *Annals of the Association of American Geographers* 92, no. 4 (2002): 662-681.

Briaud, Jean-Louis, Hamn-Ching Chen and Siyoung Park. *Predicting Meander Migration: Evaluation of Some Existing Techniques*. (2001): 2-18.

Brice, James C. "Evolution of Meander Loops." *Geological Society of America Bulletin* 85, no. 4 (1974): 581-586.

Bridge, John S. *Rivers and Floodplains: Forms, Processes, and Sedimentary Record*: John Wiley & Sons, (2009).

Brierley, Gary J and Kirstie Fryirs. "River Styles, a Geomorphic Approach to Catchment Characterization: Implications for River Rehabilitation in Bega Catchment, New South Wales, Australia." *Environmental Management* 25, no. 6 (2000): 661-679.

Brierley, Gary J and Kirstie A Fryirs. *Geomorphology and River Management: Applications of the River Styles Framework*: John Wiley & Sons, (2013).

Census.gov, "Quick Facts: Texas", 2014. http://www.census.gov/quickfacts/table/SEX255214/4866644.

Church, Michael. "The Trajectory of Geomorphology." *Progress in Physical Geography* 34, no. 3 (2010): 265-286.

Cyr, Andrew J and Darryl E Granger. "Dynamic Equilibrium among Erosion, River Incision, and Coastal Uplift in the Northern and Central Apennines, Italy." *Geology* 36, no. 2 (2008): 103-106.

Darby, Stephen E, Andrei M Alabyan and Marco J. Van de Wiel. "Numerical Simulation of Bank Erosion and Channel Migration in Meandering Rivers." *Water Resources Research* 38, no. 9 (2002): 1-21.

Data, US Climate, "Texas", 2016. http://www.usclimatedata.com/climate/texas/united-states/3213.

Deussen, Alexander. *Geology of the Coastal Plain of Texas West of Brazos River*. Vol. 126. US Government Printing Office, (1924): 1-139

Donaldson, Alan C, Richard H Martin and William H Kanes. "Holocene Guadalupe Delta of Texas Gulf Coast." *Society of Economic Paleontologists and Mineralogists: Deltaic Sedimentation, Modern and Ancient*, no. SP15 (1970): 107-137.

Dorroh, John H. "Certain Hydrologic and Climatic Characteristics of the Southwest." *University of New Mexico Publications in Engineering*. University of New Mexico Press, (1946).

Frissell, Christopher A, William J Liss, Charles E Warren and Michael D Hurley. "A Hierarchical Framework for Stream Habitat Classification: Viewing Streams in a Watershed Context." *Environmental management* 10, no. 2 (1986): 199-214.

Geist, David R. *Grays River Watershed Geomorphic Analysis*. Pacific Northwest National Laboratory (PNNL), Richland, WA, (2005): 77-83.

Gillespie, Ben M and John R Giardino. "The Nature of Channel Planform Change: Brazos River, Texas." *Texas Journal of Science* 49, no. 2 (1997): 109-142.

Godfrey, F.A. and C.L. Dowell. *Major Hydroelectric Powerplants in Texas*. Austin, Texas: Texas Water Development Board, (1968): 10.

Graf, William L. "Downstream Hydrologic and Geomorphic Effects of Large Dams on American Rivers." *Geomorphology* 79, no. 3 (2006): 336-360.

Gurnell, Angela. "Plants as River System Engineers." *Earth Surface Processes and Landforms* 39, no. 1 (2014): 4-25.

Hatch, Stephan L, Kancheepuram Natarajan Gandhi and Larry E Brown. "Checklist of the Vascular Plants of Texas." *College Station, Tex.: Texas Agricultural Experiment Station iv, En Maps Plant records. Geog* 3, (1990): 1-158.

Hickin, Edward J and Gerald C Nanson. "Lateral Migration Rates of River Bends." *Journal of Hydraulic Engineering* 110, no. 11 (1984): 1557-1567.

Holley, Edward R. "Sediment Transport in the Lower Guadalupe and San Antonio Rivers." Texas Water Resources Institute, (1992): 1-100.

Hooke, Janet. "River Meander Behaviour and Instability: A Framework for Analysis." *Transactions of the Institute of British Geographers* 28, no. 2 (2003): 238-253.

Hooke, Janet. "Complexity, Self-Organisation and Variation in Behaviour in Meandering Rivers." *Geomorphology* 91, no. 3 (2007): 236-258.

Jiang, Bin. "Head/Tail Breaks: "A New Classification Scheme for Data with a Heavy-Tailed Distribution." *The Professional Geographer* 65, no. 3 (2013): 482-494.

Knighton, David. *Fluvial Forms and Processes: A New Perspective*: Routledge, (2014): 1-52.

Konsoer, Kory M, Bruce L Rhoads, Eddy J Langendoen, James L Best, Mick E Ursic, Jorge D Abad and Marcelo H Garcia. "Spatial Variability in Bank Resistance to Erosion on a Large Meandering, Mixed Bedrock-Alluvial River." *Geomorphology* 252, (2016): 80-97.

Langbein, Walter B and Luna B Leopold. "Quasi-Equilibrium States in Channel Morphology." *American Journal of Science* 262, no. 6 (1964): 782-794.

Lee, Adam A and John R Giardino. "Rates of Channel Migration on the Brazos River." Austin, Texas: Texas Water Development Board, (2011): 1-41.

Leopold, Luna Bergere. *A View of the River*: Harvard University Press, (1994): 58.

Lewin, John. "The Lexicon of Geomorphology." *Earth Surface Processes and Landforms* 41, no. 1 (2016): 5-15.

Magilligan, Francis J and Keith H Nislow. "Changes in Hydrologic Regime by Dams." *Geomorphology* 71, no. 1 (2005): 61-78.

Montgomery, David R and John M Buffington. "Channel-Reach Morphology in Mountain Drainage Basins." *Geological Society of America Bulletin* 109, no. 5 (1997): 596-611.

Nanson, Gerald C and Edward J Hickin. "Channel Migration and Incision on the Beatton River." *Journal of Hydraulic Engineering* 109, no. 3 (1983): 327-337.

Nicoll, Tami J and Edward J Hickin. "Planform Geometry and Channel Migration of Confined Meandering Rivers on the Canadian Prairies." *Geomorphology* 116, no. 1 (2010): 37-47.

Nws.gov, "Guadalupe River at Victoria", 2016. http://water.weather.gov/ahps2/hydrograph.php?wfo=CRP&gage=VICT2.

Ouchi, Shunji. "Response of Alluvial Rivers to Slow Active Tectonic Movement." *Geological Society of America Bulletin* 96, no. 4 (1985): 504-515.

Perkin, J. S. and T.H. Bonner. "Long-Term Changes in Flow Regime and Fish Assemblage Composition in the Guadalupe and San Marcos Rivers of Texas." *River Research and Applications* 27 no.5 (2005): 566-579.

Phillips, Jonathan D. "Geomorphic Equilibrium in Southeast Texas Rivers." Texas Water Development Board, (2007): 6-103.

Phillips, Jonathan D. "Geomorphic Processes, Controls, and Transition Zones in the Guadalupe River." Austin, Texas: Texas Water Development Board, (2011): 6-68.

Phillips, Jonathan D. "Geomorphic Responses to Changes in Flow Regimes in Texas Rivers." Texas Water Development Board and Texas Instream Flow Program, (2012): 9-68.

Phillips, Jonathan D and Michael C Slattery. "Downstream Trends in Discharge, Slope, and Stream Power in a Lower Coastal Plain River." *Journal of Hydrology* 334, no. 1 (2007): 290-303.

Program, Texas Instream Flow. "Instream Flow Study of the Middle and Lower Brazos River." *Middle and lower Brazos River sub-basin study design workgroup*, (2010): 5-31.

Richard, Gigi A, Pierre Y Julien and Drew C Baird. "Statistical Analysis of Lateral Migration of the Rio Grande, New Mexico." *Geomorphology* 71, no. 1 (2005): 139-155.

Schumm, Stanley A. "Sinuosity of Alluvial Rivers on the Great Plains." *Geological Society of America Bulletin* 74, no. 9 (1963): 1089-1100.

Schumm, Stanley A, Jean F Dumont and John M Holbrook. *Active Tectonics and Alluvial Rivers*: Cambridge University Press, (2002): 8-12.

Solis, R. F. I., and F. Raul. "Upper Tertiary and Quaternary Depositional Systems, Central Coastal Plain, Texas—Regional Geology of the Coastal Aquifer and Potential Liquidwaste Repositories." *Report of Investigations* 108 (1981): 89.

Stølum, Hans Henrik. "River Meandering as a Self-Organization Process." *Science* 271, no. 5256 (1996): 1710.

Tobler, Waldo R. "A Computer Movie Simulating Urban Growth in the Detroit Region." *Economic Geography* 46, (1970): 234-240.

Wallick, Jennifer Rose, Stephen T Lancaster and John P Bolte. "Determination of Bank Erodibility for Natural and Anthropogenic Bank Materials Using a Model of Lateral Migration and Observed Erosion Along the Willamette River, Oregon, USA." *River Research and Applications* 22, no. 6 (2006): 631-649.

Winterbottom, Sandra J and David J Gilvear. "A Gis-Based Approach to Mapping Probabilities of River Bank Erosion: Regulated River Tummel, Scotland." *Regulated Rivers: Research & Management* 16, no. 2 (2000): 127-140.

Wohl, Ellen. "Floodplains and Wood." *Earth-Science Reviews* 123, (2013): 194-212.

Wolman, M Gordon and John P Miller. "Magnitude and Frequency of Forces in Geomorphic Processes." *The Journal of Geology*, (1960): 54-74.

Wolman, Markley Gordon and Luna Bergere Leopold. *River Flood Plains; Some Observations on Their Formation*. (1957): 2330-7102.